Beatrix Wieser, BSc

Regulation of Phosphoenolpyruvate Carboxykinase Expression in Lung Cancer Cells

MASTER'S THESIS

to achieve the university degree of

Master of Science

Master's degree programme: Biochemistry and Molecular Biomedical Sciences

submitted to

Graz University of Technology

Supervisor

Assoz. Prof. Priv.-Doz. Dr.rer.nat. Andelko Hrzenjak

Department of Internal Medicine, Division of Pulmonology
Medical University of Graz

Graz, July 2016

AFFIDAVIT

I declare that I have authored this thesis independently, that I have not used other than the declared sources/resources, and that I have explicitly indicated all material which has been quoted either literally or by content from the sources used. The text document uploaded to TUGRAZonline is identical to the present master‘s thesis dissertation.

Date

Signature

Danksagung

Hiermit möchte ich mich bei allen Bedanken die mich bei der Verfassung der Masterarbeit und auf dem Weg dorthin begleitet haben.

Zuerst möchte ich mich bei meinen Eltern bedanken die mich immer und in jeder Hinsicht unterstützt haben. Des Weiteren möchte ich mich auch bei Annemarie und Opa für ihre Unterstützung bedanken. Ohne euch wäre ich nie so weit gekommen!

Natürlich bedanke ich mich auch recht herzlich bei der Pulmonologie Gruppe. Besonders bei meinen Betreuern Prof. Andelko Hrzenjak und bei Dr. Katharina Leithner PhD. Durch eure Hilfe, Geduld und Unterstützung konnte ich meine Fähigkeiten weiter entwickeln und diese Arbeit schreiben.

Abstract

Lung cancer is worldwide the leading cause of cancer deaths in men and the second leading cause of cancer deaths in women. In a majority of patients lung cancer is diagnosed at an advanced stage, which is the primary reason for the high mortality rate associated with this disease. Cancer cells have many different mutations and because of that they have the potential to divide very fast. For proliferation the cells needs metabolites like glucose. Lung cancer is a rapidly growing cancer type which requires large amounts of glucose. The high consumption of glucose in proliferative cells results in reduced cellular glucose concentrations (3-10 times lower compared to normal cells). To adapt to these low glucose concentrations, cancer cells switch on metabolic pathways like gluconeogenesis using the key enzyme phosphoenolpyruvate carboxykinase (PEPCK). In eukaryotic cells two different isoforms enable the conversion of the substrate oxaloacetate to phosphoenolpyruvate, the cytosolic isoform (PEPCK-C, PCK1) and the mitochondrial isoform (PEPCK-M, PCK2). Recent studies indicate that in lung cancer cells PCK2 expression is activated under low glucose conditions. PCK2 has a unique role in cell metabolism by acting as a bottle neck in biosynthetic pathways starting from alternative carbon sources, like lactate. By inhibition or knockdown of PCK2 under glucose deprivation lung cancer cells are not viable. However, there is not much known about the regulation of PCK2 in lung cancer cells. In the liver gluconeogenesis genes can be regulated by histone deacetylases (HDACs).

Panobinostat, a histone deacetylase inhibitor that affects class I and class II HDACs, reduced the PCK2 expression in lung cancer cells. Panobinostat inhibited PCK2 expression in a concentration-dependent manner, especially under low glucose and without fetal calf serum. To get further information about the regulation of PCK2, we performed silencing experiments with specific HDAC siRNAs. HDAC3 silencing led to a lower PCK2 expression under starvation conditions. These results provide a better understanding of the metabolism of human lung cancer cells.

Kurzfassung

Lungenkrebs ist die häufigste Krebs-Todesursache bei Männern und die zweit häufigste bei Frauen. Die Diagnose wird in den meisten Patienten erst in einem späten Stadium der Erkrankung festgestellt. Tumorzellen haben verschiedene Mutationen durch die es ihnen möglich ist sich ständig zu teilen. Für diesen Prozess braucht die Zelle Metaboliten wie zum Beispiel Glukose. Lungenkrebs ist eine sehr schnell wachsende Krebs Art und benötigt daher viel Glukose. Deshalb ist die Glukose Konzentration in Lungenkrebszellen 3 bis 10 mal geringer als in gesunden proliferierenden Zellen. Um sich an diese Bedingungen anzupassen und genug Metaboliten für weitere Zellteilungen zu bekommen, beginnt die Tumorzelle mit Glukoneogenese. Ein Schlüsselenzym in diesem Prozess ist die Phoshoenolpyruvat Carboxykinase (PEPCK). Von diesem Enzym gibt es zwei Isoformen, welche die Umwandlung von Oxalacetat in Phosphoenolpyruvat katalysieren: eine cytoplasmatische Isoform (PEPCK-C, PCK1) und eine mitochondriale Isoform (PEPCK-M, PCK2). Neueste Studien zeigen, dass PCK2 unter geringer Glukose Konzentration in Lungenkrebszellen aktiviert wird. PCK2 ist ein essentielles Enzym für Lungenkrebszellen unter geringen Glukose Bedingungen, da die Zellen dadurch aus alternativen Kohlenstoffquellen, wie Laktat, neue Metaboliten erzeugen. Wenn die Tumor Zelle nur geringe Glukose Mengen zur Verfügung hat und PCK2 inhibiert wird, ist diese Zelle nicht lebensfähig. Jedoch ist wenig über die Regulation von PCK2 in Lungenkrebs bekannt. Glukoneogenese Gene, wie PCK2, werden in der Leber unter anderem mittels Histon Deaceytlasen (HDACs) reguliert. Mit Panobinostat, einem HDAC Klasse I und II Inhibitor, konnte die PCK2 Expression in Lungenkrebs Zellen reduziert werden. Vor allem unter geringen Glukose Bedingungen und ohne fetalem Kälber Serum konnten konzentrationsabhängige Effekte beobachtet werde. Des Weiteren konnte durch silencing von HDACs gezeigt werden, dass HDAC3 eine wichtige Rolle in der Regulation von PCK2 spielen könnte. Diese Ergebnisse führen zu einem besseren Verständnis der Regulation von menschlichen Lungenkrebszellen.

Table of Contents

1. Introduction

1.1. Lung cancer

Lung cancer occurs by genomic changes in pulmonary cells (Sekido et al., 2003). Unlimited proliferation and resistance to apoptosis caused by epigenetic or genetic changes can lead to tumor growth (Hanahan et al., 2011). Mutations in tumor cells enable them to change their metabolism in order to allow rapid proliferation. These processes are especially characteristic for malignant tumors (Waclaw et al., 2015). Before the 20th century lung cancer was a rare disease, but at the end of the last century it became one of the leading causes of cancer death. The exposure to new etiologic agents like air pollution, manufactured cigarettes, passive smoking, an extended lifespan and many substances like arsenic, nickel, asbestos and chromates makes lung cancer a frequent disease (Alberg et al., 2003). Nowadays lung cancer is the leading cause of cancer death worldwide (Alberg et al., 2013; Ramalingam et al., 2011) and 18% of the total number of deaths can be traced back to this type of cancer. Thirteen percent of newly diagnosed cancers worldwide is lung cancer (Koinis et al., 2016) and 80% of the patients already have metastasis at the time of diagnosis, which is one of the mean reasons for the high mortality rate (Polanski et al., 2016; Ramalingam et al., 2011).

Based on their histological characteristics, there are two different types of lung cancer: Non-small cell lung cancer (NSCLC) and small cell lung cancer (SCLC) (Hanna et al., 2013). The biology, response to therapy, and prognosis is different for these two types (Roviello, 2015). About 15% of the diagnosed lung tumors are SCLC (Polanski et al., 2016; Ramalingam et al., 2011). SCLC is an aggressive tumor with bad prognosis which is strongly correlated with smoking. SCLC grows very fast and forms metastasis at an early stage (Koinis et al., 2016). Eighty-five percent of the diagnosed lung cancers are NSCLC (Polanski et al., 2016; Ramalingam et al., 2011). There are three histological subtypes of NSCLC: adenocarcinoma, large cell carcinoma and squamous cell carcinoma (Herbst et al., 2008). The most frequent type of NSCLC is the adenocarcinoma (Roviello, 2015). Adenocarcinoma develops from small bronchioles, bronchi, or alveolar epithelial cells and is the predominant type in patients who never smoked. Our experiments within this project were done by using the human

adenocarcinoma cell line A549 (Murakami, 2002).

1.2. Nutrient uptake and Warburg effect

Mammalian cells have control systems for nutrient uptake to prevent uncontrolled cell proliferation. However, cancer cells can overcome these systems with oncogenic mutations. They have a permanent nutrient uptake that promotes cell growth. The preferred nutritional molecule is glucose because it is necessary for cell proliferation. In differentiated tissue glucose is metabolized to pyruvate by glycolysis (Vander Heiden et al., 2009) and then enters the tricarboxylic acid (TCA) cycle (Polet et al., 2013). Glycolysis consumes two molecules of adenosine 5′-triphosphate (ATP) and produces four ATPs which results in a positive ATP balance. Pyruvate is transported from the cytoplasm to the mitochondria and converted into acetyl-coenzyme A (acetyl-CoA) and CO_2. Acetyl-CoA enters the citric acid cycle and is fully oxidized to CO_2 and H_2O (Li et al., 2015), generating NADH under aerobic conditions (Bender et al., 2016). The NADH generated by the acidic cycle is used by the electron transport chain to provide energy (Crawford et al., 2016). This process is called oxidative phosphorylation and generates 36 mol ATP by using only one mol of glucose. If O_2 is not available cells switch their metabolism to anaerobic glycolysis, where lactate is generated from glucose. With this step glycolysis can be continued but only with a minimal ATP production compared to oxidative phosphorylation. The cell can only generate 2 mol ATP by using one mol of glucose (Figure 1) (Vander Heiden et al., 2009).

Cancer cells prefer anaerobic glycolysis even if O_2 is present. This phenomenon is called the Warburg effect and is named after Otto Warburg. Ten percent from the glucose is used for biosynthetic pathways upstream the pyruvate production (Figure 1) (Vander Heiden et al., 2009). Glycolytic intermediates can be shuttled into the pentose phosphate pathway to produce reduced nicotinamide adenine dinucleotide phosphate (NADPH) or ribose. NADPH is important for the redox balance and a well-adjusted redox balance supports fast tumor growth. Altogether the produced intermediates are used to synthesize nucleotides, carbohydrates, proteins and lipids (Figure 2) (Cairns et al., 2011).

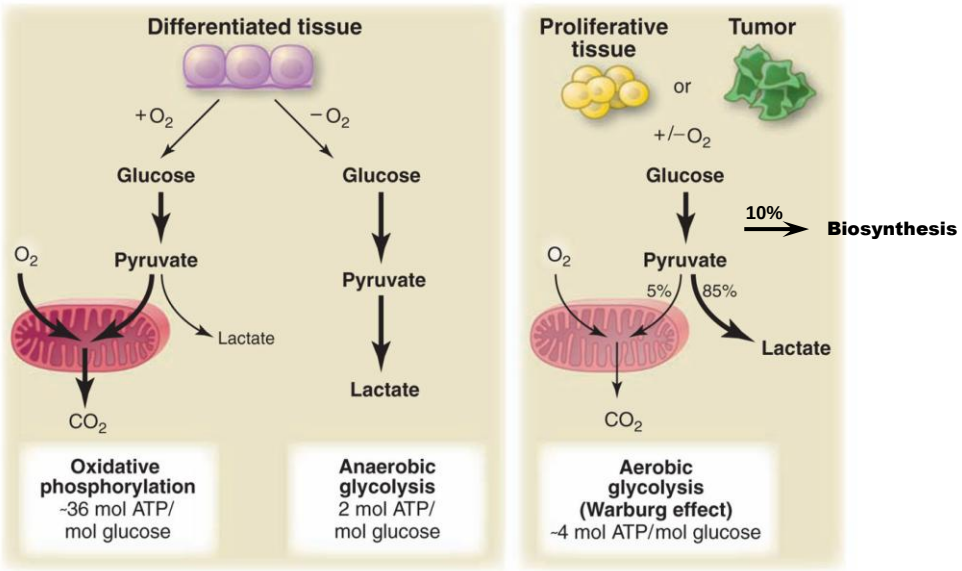

Figure 1: Overview of glycolysis in differentiating cells and in tumor cells. The differences between oxidative phosphorylation, anaerobic glycolysis, and the Warburg effect are shown. In differentiated cells and in presence of O_2 the glucose is metabolized primary by oxidative phosphorylation to CO_2. This process takes place in cytoplasm and in mitochondria. The cell can generate about 36 mol ATP from one mol glucose. If O_2 is limited, glucose is metabolized to lactate by anaerobic glycolysis. By this the cell generates only two mol ATP from one mol glucose. Otto Warburg observed 1924 that cancer cells metabolize glucose in a different way than differentiated cells. Although O_2 is present, cancer cells produce ATP preferentially via aerobic glycolysis. Only 5% of the glucose is transported into mitochondria and can be used by oxidative phosphorylation. Ten percent of the glucose is used for biosynthesis upstream of pyruvate production (modified from Vander Heiden et al., 2009).

There is no exact explanation for the Warburg effect but it is obvious that this effect is an advantage for tumor cells (Li et al., 2015). A possible explanation for the switch to aerobic glycolysis is the need for glycolytic intermediates to support biosynthesis (Liberti et al., 2016). Furthermore, generation of lactate leads to an acidic environment in the cell. Cancer cells need an alkaline intracellular milieu; therefore the cell has to shuttle out the lactate. The excretion of the lactate generates an acidic milieu outside of the cell. This may support cancer cell invasion and metastasis formation (Schulze et al., 2012).

Glutamine is also an important fuel for cancer cells. Glutamine can be metabolized to non-essential amino acids and glutathione (GSH). Glutamine can be also metabolized to α-ketoglutarate and can enter the TCA cycle (Figure 2) (Cantor et al., 2012).

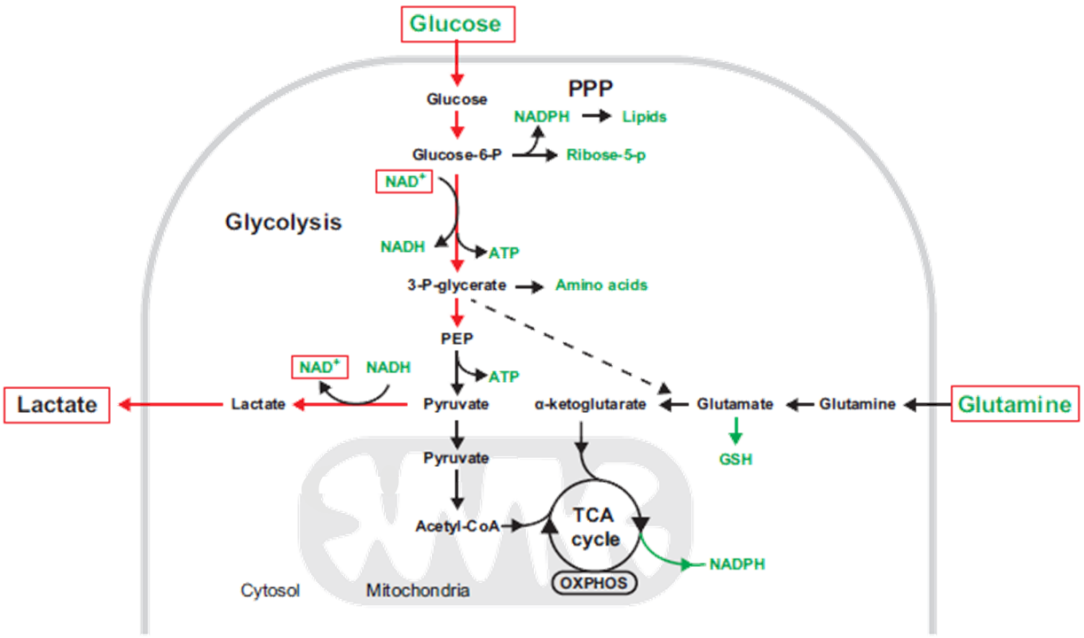

Figure 2: Glucose and glutamine metabolism. Glycolysis generates nicotinamide adenine dinucleotide (NADH) and adenosine 5′-triphosphate (ATP) but also other intermediates that are used for numerous biosynthetic pathways. The end product of glycolysis is pyruvate. Transformation from pyruvate to lactate reduces NADH to NAD^+ which is important for the glycolytic flux. The pentose phosphate pathway (PPP) starts from glucose-6-phosphate (glucose-6-p) and generates NADPH, amino acids and molecules for DNA and lipid synthesis. Pyruvate can be metabolized to acetyl-coenzyme (acetyl-CoA) and is used in the tricarboxylic acid (TCA) cycle that provides NADH and also metabolic intermediates. Glutamine uptake can refuel the TCA cycle. Oxidative phosphorylation (OXPHOS) and TCA cycle are coupled to allow a high proliferation rate. glutathione (GSH), phosphoenolpyruvate (PEP) (modified from Polet et al., 2012).

1.3. Gluconeogenesis

Cancer cells need an extraordinary high amount of glucose. This demand cannot be delivered only with the blood flow (Leithner et al., 2015). Glucose concentration in tumors can be 3 to 10 times lower than in healthy tissue. This deficit of glucose leads to metabolic stress in cancer cells. Glutamine can be used for the TCA cycle and for Acetyl-CoA production. However, this is not enough for the high amount needed in cancer cells (Vincent et al., 2015). So there is a further mechanism necessary: under low glucose concentration lactate is metabolized to pyruvate. Pyruvate can be shuttled into the mitochondria for Acetyl-CoA production as descried before (Li et al., 2015) or can be used for glucose production. The biochemical process from pyruvate to glucose is called gluconeogenesis (Han et al., 2016). Several steps of glycolysis

and gluconeogenesis are similar but there are also some steps included which are unique for the gluconeogenesis (Wallace et al., 2002). One of this unique steps is catalysed by a key regulatory enzyme in gluconeogenesis which is the phosphoenolpyruvate carboxykinase (PEPCK) (Xiong et al., 2011). PEPCK catalyzes the conversion from oxaloacetate to phosphoenolpyruvate. To catalyze this reaction, the phosphate donor guanosintriphosphat (GTP) is necessary. All eukaryotes have two isoforms of PEPCK; a cytosolic (PEPCK-C, PCK1) and a mitochondrial (PEPCK-M, PCK2) (Yang et al., 2009). Under low glucose conditions the production of phosphoenolpyruvate is important for the tumor cell growth and proliferation (Vincent et al., 2015). Recent studies indicated that PCK2 expression is activated under low glucose conditions in lung cancer cells. In these cells, which were cultured under low glucose, lactate is converted to pyruvate and then to phosphoenolpyruvate by PCK2. Thus PCK2 is an important factor for lung cancer cells under low glucose conditions (Leithner et al., 2015). Glutamine can also be used to produce phosphoenolpyruvate via PCK2 (Vincent et al., 2015). There are different potential pathways for the produced phosphoenolpyruvate. Phosphoenolpyruvate can be metabolized to ribose-5-phosphate in the pentose phosphate pathway. An alternative reaction would be the conversion to glycerol for lipid synthesis or synthesis of glucose-6-phosphate. Phosphoenolpyruvate synthesis is dependent on the cellular needs and maybe also on the type of the tumor. Long time it was unknown that lung cancer cells utilize gluconeogenesis (Leithner, 2015). It was established that only a few cell types like liver, adipocytes, intestine and kidney exhibit gluconeogenesis (Méndez-Lucas et al., 2014). It has been shown that in NSCLC tumors PCK2 expression is upregulated. PCK2 is important for the glucose independent cell growth (Vincent et al., 2015) and it might be potential target for cancer therapy (Leithner, 2015).

1.4. Regulation of gluconeogenesis

Insulin regulates the induction of gluconeogenesis; after feeding there is more insulin present (no gluconeogenesis is necessary) than under fasting conditions. Under feeding conditions insulin activates the transmembrane insulin receptor (IR) tyrosine kinase. This kinase phosphorylates the insulin

receptor substrate (IRS). The next enzyme in this pathway is class 1A phosphatidylinositol 3-kinase (PI3K) which is stimulated by IRS to produce phosphatidylinositol (3,4,5)-triphosphate (PIP), and recruits the 3-phosphoinositide dependent protein kinase-1 (PDPK1) and AKT. PDPK1 phosphorylates AKT which phosphorylates FOXO1 (forkhead box protein 1) directly and CREB regulated transcription coactivator 2 (CRTC2) indirectly. Thereby the transcription of gluconeogenesis genes is suppressed (Figure 3). During fasting the IR–IRS-PI3K-PDPK1-AKT pathway is less active because there is a lower insulin amount that cannot activate the IR. FOXO1 and CRTC2 are not phosphorylated and can be shuttled into the nucleus. The cAMP response element-binding protein (CREB), CRTC2, CREB binding protein (CBP) complex and FOXO1 bind to the DNA and transcription of genes involved in gluconeogenesis is induced (Figure 3) (Cheng et al., 2012).

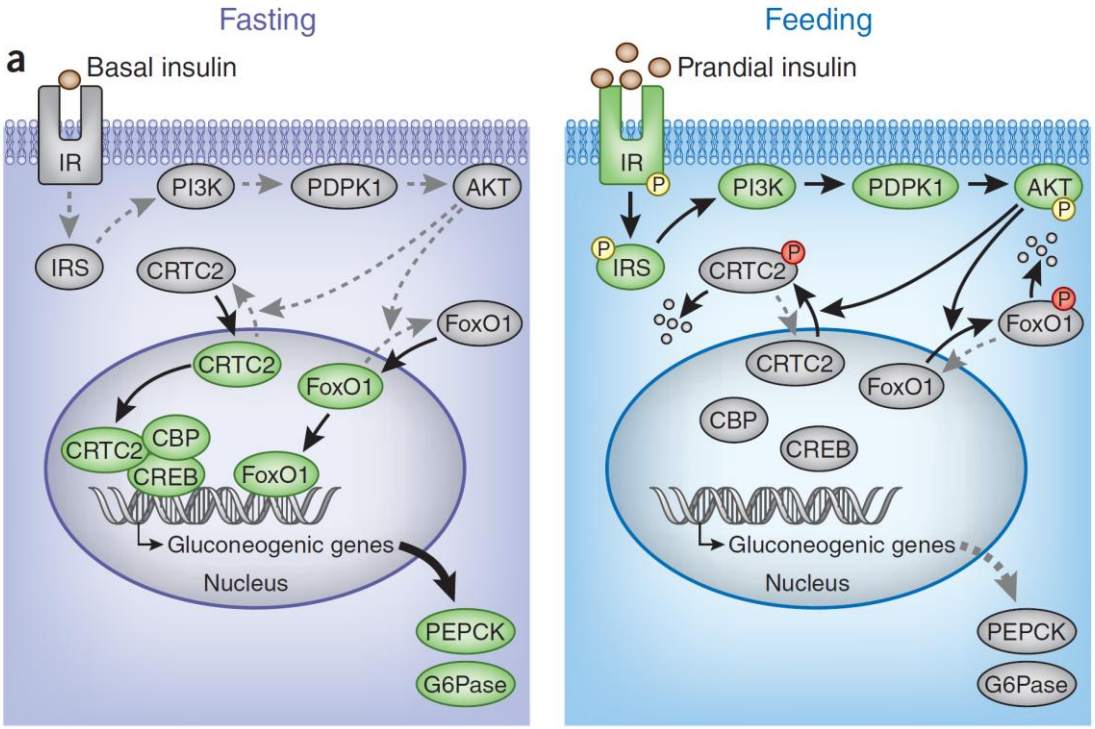

Figure 3: Gluconeogenesis regulation is mediated by insulin. Under fasting conditions the IR–IRS-PI3K-PDPK1-AKT pathway is less active. Gluconeogenesis can start by FOXO1 and CREB-CBP-CRTC2 complex binding to DNA. Under feeding conditions insulin activates IR–IRS-PI3K-PDPK1-AKT pathway and FOXO1 and CRTC2 are inactivated by phosphorylation. Insulin receptor (IR), insulin receptor substrate (IRS), phosphatidylinositol 3-kinase (PI3K), 3-phosphoinositide dependent protein kinase-1 (PDPK1), cAMP response element-binding protein (CREB), CREB regulated transcription coactivator 2 (CRTC2) and CREB binding protein (CBP), phosphoenolpyruvate carboxykinase (PEPCK), glucose-6-phosphatase (G6Pase) (Cheng et al., 2012).

1.5. Histone deacetylases

Mihaylova et al showed that histone deacetylases (HDACs) plays a role in the regulation of gluconeogenesis is the liver (Mihaylova et al., 2011). HDACs are enzymes which cleave lysine residues from histones and from many other proteins by deacetylation. The acetylation is accomplished by histone acetyltransferases (HATs). Histones are important to pack the DNA in a compact form called chromatin. Thereby, DNA is wrapped around the histone core which consists of two copies of four different histones (H2A, H2B, H3, and H4), thus forming an octamer (Lu et al., 2015; Cheung et al., 2005). Histone (H1) is used to pack the DNA in a more compact form called nucleosome (Cheung et al., 2005).

The acetylation by HATs brings a negative charge to the positively charged lysine residues from the histone complex. Now DNA and histones are both negatively charged, which leads to repulsion so the chromatin complex opens and the DNA is accessible for transcription factors (Figure 4) (Lu et al., 2015). Deacetylation has the opposite effect: the negative charge is removed by HDACs, the chromatin complex is condensed and the transcriptional activation is reduced (Figure 4) (Mihaylova et al., 2013).

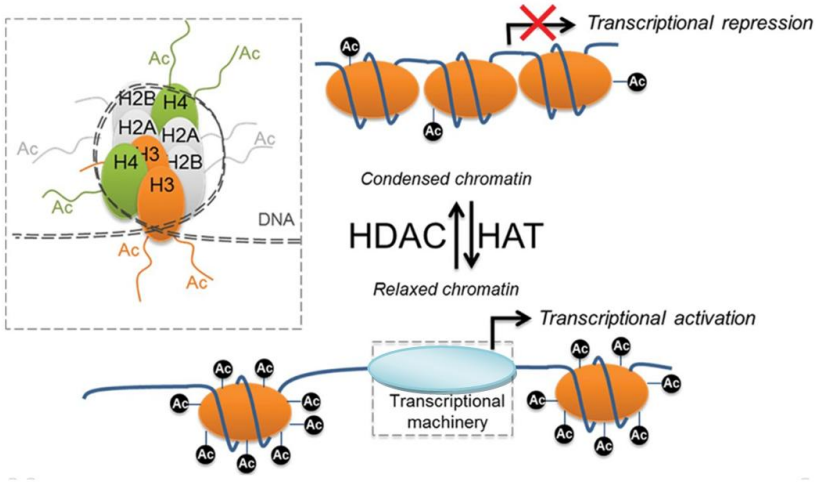

Figure 4: Histone acetylation and deacetylation. The histone core consists of two copies from each histone (H2A, H2B, H3, and H4). The DNA is wrapped around this protein complex. If HATs acetylate this complex the DNA histone binding is relaxed and the transcription machinery can bind to the DNA - the transcription can start. HDACs have the opposite effect, they remove the negative charge from the histones, the chromatin complex is tightly packed and the transcription stops (modified from Whittle et al., 2014).

HDACs are highly conserved and can be divided into HDAC class I, II, III and IV HDACs from different classes have different functions and structures (Haberland et al., 2009). Class I, II and IV have all a zinc ion to catalyze the deacetylation of the lysine residues (Holbert, 2005). Class III HDACs belongs to the second group containing NAD^+-dependent proteins called sirtuins, and will not be discussed here in detail (Mihaylova et al., 2013). HDACs from class I and II can deacetylate not only histones but also non histone proteins like transcription factors or coactivators. This acetylation can enhance or inhibit their activity (Mihaylova et al., 2013).

HDAC1, 2, 3 and 8 belong to class I and have all a HDAC domain (Figure 5). HDAC1 and 2 have often a similar function and can act as transcriptional repressors. HDAC3 can activate transcription by interaction with an enzyme complex. This complex assembles from nuclear receptor corepressor (NCoR1) and silencing mediator of retinoic and thyroid receptors (SMRT/NCoR2). The NCor/SMRT complex recruits HDAC3 to the promoter. Once HDAC3 is bound to NCor/SMRT it can interact with HDAC class IIa enzymes. Under fasting conditions class IIa HDACs are activated and stimulate the HDAC3/NCoR complex which deacetylate FOXO (Mihaylova et al., 2013). FOXO transcription factors play an important role in the regulation of cellular processes (Urbánek et al., 2016). After deacetylation of FOXO by HDAC3, FOXO can bind to the DNA and the transcription is initiated (Figure 6) (Mihaylova et al., 2013).

The HDAC class II is divided in two subclasses: class IIa (HDAC4, 5, 7, 9) and IIb (HDAC6 and HDAC10). The HDAC domain in the C-terminus of class IIa is highly conserved. The N-terminal domain contains phosphorylation sites and protein binding domains (Figure 5). Class IIa HDACs is the only class which can be exported and imported into the nucleus. This transport is regulated by phosphorylation of serine residues. After the phosphorylation the HDACs bind to 14-3-3 adapter proteins and so they are shuttled out of the nucleus. HDAC6 from the class IIb has two HDAC domains and an ubiquitin biding domain. HDAC10 has a leucine rich domain at the C-terminus but there is not much known about class IIb HDACs (Figure 5) (Mihaylova et al., 2013).

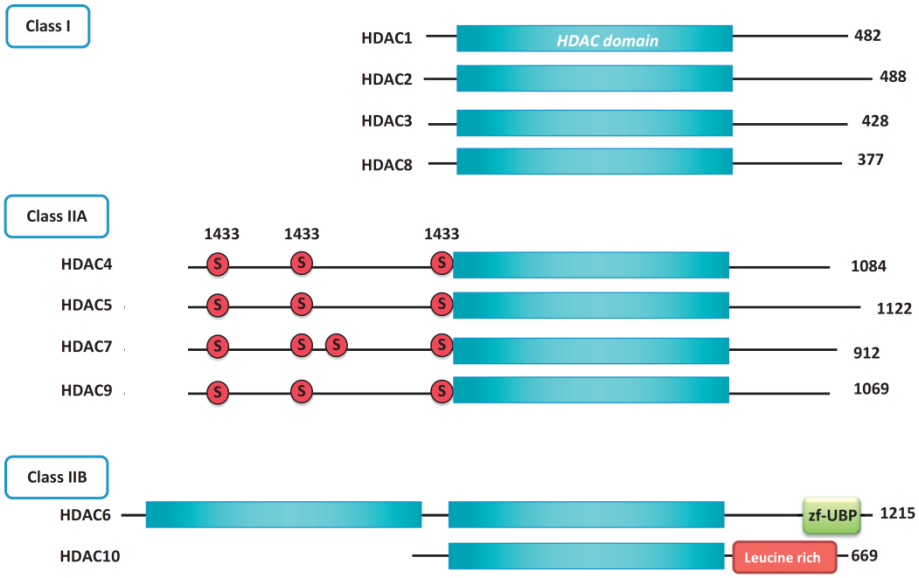

Figure 5: Structure of class I and II HDACs. All class I and class II HDACs have a highly conserved HDAC domain (blue boxes). On the N-terminal domain serines (red S) are located which can be phosphorylated and interact then with 14-3-3 binding proteins. HDAC6 is the only HDAC with two HDAC domains. HDAC6 has a zinc-finger ubiquitin-binding domain (zf-UBP). HDAC10 has a leucine rich region and also a HDAC domain (modified from Mihaylova et al., 2013).

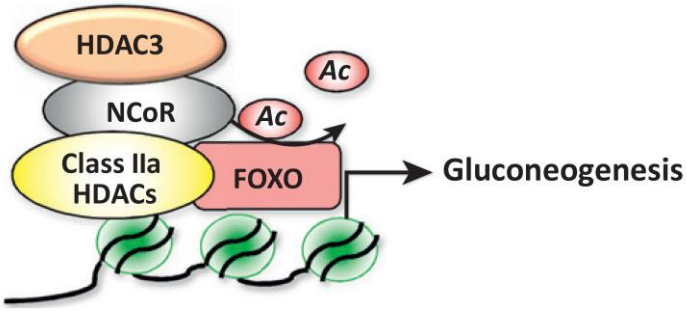

Figure 6: Interplay of gluconeogenesis genes with HDACs. Under fasting conditions class IIa HDACs get active and recruit the HDAC3/NCoR complex. HDAC3 deacetylates the transcription factor FOXO. FOXO can bind to the DNA and the transcription of the gluconeogenesis genes starts (Mihaylova et al., 2013).

1.5.1. HDAC inhibitors

Different HDAC inhibitors lead to a high acetylation of histones and non-histone proteins. This frequently leads to cell cycle arrest and apoptosis in cancer cells (Bailey et al., 2015). One of these substances frequently used for research purposes and in preclinical studies is panobinostat (LBH589) (Fischer et al., 2015; Laubach et al., 2015). Panobinostat is a nonselective HDAC inhibitor for class I and II HDACs (Laubach et al., 2015; Bailey et al., 2015). Panobinostat

shows cytotoxic activity against tumor cells, whereas the cytotoxic effects on healthy cells are limited (Bailey et al., 2015). The half maximal inhibitory concentrations (IC_{50}) for panobinostat is usually in low nanomolar (nM) range (Laubach et al., 2015). The combination of panobinostat and radiation showed an growth delay in human NSCLC nude mice xenografts (Anne et al., 2013). In preclinical studies panobinostat showed positive effects in multiple myeloma, chronic myeloid leukemia, cutaneous T-cell lymphoma, myeloid leukemia and some solid tumors (Bailey et al., 2015).

Preliminary experiments showed that panobinostat had an influence on the amount of PCK2 mRNA in A549 lung cancer cells. At the highest panobinostat concentration (128 nM), the PCK2 mRNA amount was tentatively lower than without panobinostat (Figure 7) (Leithner K. unpublished data).

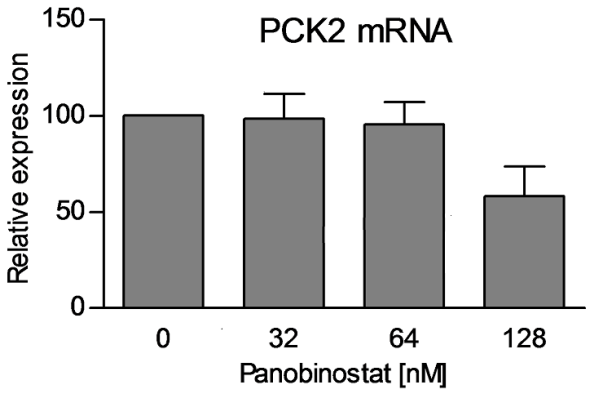

Figure 7: Impact of panobinostat on PCK2 mRNA level in A549 cells. Cells were cultivated in DMEM/F12 complete and treated with different concentrations of panobinostat for 24 hours. Then the PCK2 mRNA levels were analyzed by quantitative real-time polymerase chain reaction (qPCR). Beta-actin was used as a reference gene (Leithner, unpublished data).

2. Aims

The central aim was to learn more about the regulation of PCK2 under different environmental conditions. So we performed different experiments to analyze the regulation of PCK2.

- Investigation of the inhibition of HDACs with panobinostat (HDAC class I and II inhibitor) in A549 cells.
- Silencing of different HDACs in A549 lung adenocarcinoma cells.
- Treatment of A549 cells with HDACs inhibitors and analysis of the PCK2 expression.

3. Materials and Methods

3.1. General solutions

Table 1: General reagents used in this study.

Compound	Manufacturer
Acrylamide 30%	Merck, Darmstadt, Germany
Agarose	BioRad Industries, Hercules CA
ECL Prime Western Blotting Detection Reagent	GE Healthcare, Little Chalfont, GBR
Hyperfilm ECL high performance chemiluminescence film	GE Healthcare, Little Chalfont, GBR
Ammonium persulfate	Sigma Aldrich, Vienna, Austria
β-mercaptoethanol	Sigma Aldrich, Vienna, Austria
Bicinchononic Acid Protein Assay Kit (BCA)	(Novagen, Wisconsin, USA)
Bovine Serum Albumin (BSA)	Roth, Karlsruhe Germany
Bromophenol Blue	Sigma Aldrich, Vienna, Austria
CellEvent™ Caspase-3/7 Green Detection Reagent kit	Thermo Scientific, Fremont, USA
D-(+)-Glucose monohydrate	Sigma Aldrich, Vienna, Austria
DMEM/F12	Gibco, Paisley, UK
DMEM 1x	Gibco, Paisley, UK
Dimethylsulfoxide (DMSO)	Sigma Aldrich, Vienna, Austria
Ethanol	Merck, Darmstadt, Germany
Fetal calf serum (FCS)	Biowest, Nuaillé, France
Glacial Acetic Acid	Sigma Aldrich, Vienna, Austria
Glycerol	Sigma Aldrich, Vienna, Austria
Glycine	Sigma Aldrich, Vienna, Austria
iScript™ cDNA Synthesis Kit	BioRad Industries, Hercules CA
Jet Prime® kit	Polyplus-transfection, Illkirch-Graffenstaden, France
L-Glutamine 200mM	Gibco, Paisley, UK
LMK235, N-[[6-(Hydroxyamino)-6-oxohexyl]oxy]-3,5-dimethylbenzamide	Tocris Bioscience, Avonmouth, Bristol, GBR
Methanol	Merck, Darmstadt, Germany
Milk powder	Roth, Karlsruhe Germany
Sodiumchloride (NaCl)	Roth, Karlsruhe Germany
Nitrocellulose Membrane	BioRad Industries, Hercules CA
Panobinostat	LC, Laboratories, Woburn, MA
peqGOLD® Total RNA Kit	Peqlab, Erlangen, Germany
PeqGreen	VWR, Radnor, Pennsylvania
Phenolred	Sigma Aldrich, Vienna, Austria
Phosphatase Inhibitor	Thermo Scientific, Fremont, USA
Phosphate Buffered Saline (PBS) pH 7,4	LKH Graz pharmacy
peqGOLD® Total RNA Kit	Peqlab, Erlangen, Germany
Polyvinylidene Difluoride Membrane (PVDF)	GE Healthcare, Little Chalfont, GBR

Table 1: General reagents used in this study (continued).

Ponceau-S	Merck, Darmstadt, Germany
Proteinase Inhibitor	Thermo Scientific, Fremont, USA
Protein™ Standard Dual Color	BioRad Industries, Hercules CA
QuantiFast SYBR PCR kit	Qiagen, Venlo, Netherlands
Restore PLUS Western Blot stripping Buffer	Thermo Scientific, Fremont, USA
RGFP966	MedChem Expres, Princeton, NJ, USA
RIPA Buffer	Sigma Aldrich, Vienna, Austria
Sodium Dodecyl Sulfate (SDS)	Sigma Aldrich, Vienna, Austria
Super Signal WesternPico Chemiluminescent Substrate	Thermo Scientific, Fremont, USA
TAE	LKH Graz pharmacy
N,N,N',N'-Tetramethylethylendiamin (TEMED)	Sigma Aldrich, Vienna, Austria
T-MAT, G/RA film	Carestream Health, Rochester, NY
Trizma base	Sigma Aldrich, Vienna, Austria
Trizma HCl	Sigma Aldrich, Vienna, Austria
0.25% Trypsin-EDTA	Gibco, Paisley, UK
100 U/ml penicillin	Gibco, Paisley, UK
100 µg/ml streptomycin	Gibco, Paisley, UK

3.2. Buffers and solutions

Table 2: Buffers and solutions used in this study.

Buffer	Ingredient
10x TBS	31.5 g Trizma HCl 80 g NaCl add aqua dest. to one liter adjust to pH 7.5
TBS-T	100 ml 10x TBS 900 ml aqua dest. 0.1% Tween 20
10x running buffer	30 g Trizma base 144 g glycine 100 ml SDS add to one liter aqua dest.
1x running buffer	100 ml running buffer 900 ml aqua dest.
10x transfer buffer	56 g Trizma Base 286 g glycine add aqua dest. to two liter
1x transfer buffer	100 ml 10x transfer buffer 200 ml methanol 700 ml aqua dest.

Table 2: Buffers and solutions used in this study (continuation).

5x Laemmli buffer	30 mM Tris HCl pH 6.8 2% sodium dodecyl sulfate 10% glycerol 5% β-mercaptoethanol 0.01% bromophenol blue
Ponceau-S-red	0.5 g Ponceau-S 98.5 ml aqua dest. 1 ml glacial acetic acid 10 ml RIPA buffer
Lysis Buffer	1 Proteinase Inhibitor 1 Phosphatase Inhibitor
1.5 M Tris	210.6 g Trizma HCl 20.1 g Trizma Base add 1 l aqua dest. adjust to pH 6.8
1.0 M Tris	36.9 g Trizma HCl 153.9 g Trizma base add aqua dest. to one liter adjust to pH 8.8

3.3. Gels

3.3.1. Agarose gel

Table 3: Compounds for 100 ml 3% agarose gel.

Reagenz	3% gel
Agarose	3 g
1x TAE	97 g
PeqGreen	5 µl

3.3.2. Resolving gel

Table 4: Ingredients for two resolving gels 8% or 10%.

Reagenz	8% gel	10% gel
Aqua dest.	9.2 ml	7.9 ml
30% Acrylamide	5.2 ml	6.7 ml
1.5 M Tris pH 8.8	5.2 ml	5 ml
10% SDS	200 µl	200 µl
10% APS	200 µl	200 µl
TEMED	12 µl	8 µl

3.3.3. Stacking gel

Table 5: Solutions for two stacking gels (4.5%).

Reagenz	
Aqua dest.	6.8 ml
30% Acrylamide	1.66 ml
1.5 M Tris pH 8.8	1.26 ml
10% SDS	100 µl
10% APS	100 µl
TEMED	10 µl

3.4. Antibodies

For all antibodies listed in Table 6 the membranes were blocked in 5% milk-TBST solution (MTBST) and the primary antibodies were also diluted in MTBST. Only the PCK2 antibody was diluted in 5% BSA-TBST. Both, blocking and dilution for HDAC2 antibody was done in BSA.

Table 6: Antibodies used in this study.

Primary antibody	Dilution	Catalogue no.	Manufacturer
Acetylated HDAC3	1:1000	sc-8655_R	Santa Cruz
Acetylated HDAC4	1:1000	sc-8660-R	Santa Cruz
beta-actin	1:3000	447778	Santa Cruz
HDAC1	1:5000	PA1-860	Thermo Scientific
HDAC2	1:1000	#2540S	Cell Signaling
HDAC3	1:1000	7G6C5	Thermo Scientific
HDAC4	1:1000	#2072	Cell Signaling
HDAC5	1:1000	sc-133225	Santa Cruz
HDAC6	1:1000	sc-28386	Santa Cruz
PCK2	1:500	ab77047	Abcam

Secondary antibody	Dilution	Catalogue no.	Company
anti-mouse-HRP	1:20000 for PCK2 1:2000 for HDAC3, 5 and 6	sc-2005	Santa Cruz
anti-rabbit-HRP	1:2000	#7074	Cell Signaling

3.5. QPCR primer

Table 7: QPCR primer sequences.

Gene	Sequence
beta-actin F	5´-ATTGCCGACAGGATGCAGGAA-3´
beta-actin R	5´-GCTGATCCACATCTGCTGGAA-3´
beta-2 microglobulin F	5´-GCCTGGAGGCTATCCAGCGTACT-3´
beta-2 microglobulin R	5´-CCATTCTCTGCTGGATGACGTGAGT-3´
HDAC1 F	5´-AGTGCGGTGGTCTTACAGTG-3´
HDAC1 R	5´-CACACTTGGCGTGTCCTTTG-3´
HDAC2 F	5´-TTCAGTTGCTGGAGCTGTGA-3´
HDAC2 R	5´-AGCATGATGTAATCCTCCAGCC-3´
HDAC3 F	5´-GCATGGGGAATGGGT-3´
HDAC3 R	5´-TCTCATATGTCCAGCAGG-3´
HDAC4 F	5´-CCACCTCACTCCCTACCTGA-3´
HDAC4 R	5´-CCCAGGCCTGTGACGAG-3´
HDAC5 F	5´-CAACGAGTCGGATGGCATGT-3´
HDAC5 R	5´-ATGCTGTGCAGAGAAGTCCG-3´
HDAC6 F	5´-GCGGAGTGGAAGAACCG-3´
HDAC6 R	5´-CTACTTCTTCGCTGCCTGGT-3´
PCK2 F	5´-CATCCGAAAGCTCCCCAAGTA-3´
PCK2 R	5´-TGGAAATCAGCTGGGGACATC-3´

All qPCR primers were purchased from Eurofins Genomic. F, forward; R, reverse.

Table 8: PCR product length for different HDACs.

HDAC	product lenght [bp]
HDAC1	91
HDAC2	79
HDAC3	107
HDAC4	120
HDAC5	72
HDAC6	92

3.6. SiRNAs

Table 9: siRNAs used in this study.

Targe gene	Catalogue no.	Manufacturer
HDAC1	L-003493-00-0005	Dharmacon
HDAC2	L-003495-02-0005	Dharmacon
HDAC3#1	L-003496-00	Dharmacon
HDAC3#2	sc-35538	Santa Cruz
HDAC4	L-003497-00-0005	Dharmacon
HDAC5	L-003498-00-0005	Dharmacon
HDAC6	L-003499-00-0005	Dharmacon
Control si	D-001810-01-05	Dharmacon
Control si	sc-37007	Santa Cruz

3.7. Cell culture

3.7.1. Medium preparation

For standard conditions A549 cells were cultured in DMEM/F12 with 100 U/ml penicillin, 100 µg/ml streptomycin, 2 mM glutamine and 10% dialyzed, heat-inactivated FCS (FCS), further referred as DMEM/F12 complete.

Glucose and FCS starvation media were prepared as follows: glucose- and glutamine- free DMEM medium was supplemented with 100 U/ml penicillin, 100 µg/ml streptomycin, 1 mM glutamine and phenol red. Media with 20 mM D-glucose and without glucose were prepared by adding D-(+)-glucose monohydrate and filtering through 0.22 µm filters. These two media were mixed to obtain concentrations of 0.2, 1 and 10 mM glucose. Dialyzed calf FCS was added as appropriate. Medium containing 0.2 mM glucose and no FCS is further referred as starvation medium and medium containing 10 mM glucose and 10% FCS is called non-starvation medium.

3.7.2. Cultivation of A549 cells

Human A549 lung adenocarcinoma cells used in this study were purchased from Cell Lines Service (Eppelheim, Germany). Cells were cultured at 37°C under 5% CO_2 and 98% humidity.

To detach cells from the culture flasks cells were washed with phosphate-buffered saline (PBS) and trypsinized with 3 ml 0.25% Trypsin-EDTA. Trypsin-EDTA enzymatically degrades the proteins which are important for cell attachment to the surface. After five minutes 7 ml medium containing 10% FCS was added to the cells to stop the trypsin activity. The cell suspension was centrifuged for 5 minutes at 400 g and the supernatant was discarded. The cell pellet was resuspended in DMEM/F12 complete. To count the cell number an electronic pulse area analysis system was used (CASY®, Innovartis, Reutlingen, Germany). For the measurement the cell suspension was diluted 1:200 with Casyton.

3.7.3. Glucose concentration series

A stock solution of 500 mM glucose was prepared by dissolving glucose in aqua dest. This solution was filtered with a 0.22 µm filter. A549 cells (200,000/well)

were plated in DMEM/F12 complete. After 24 hours cells were washed twice with PBS and incubated in DMEM media with different glucose concentration with or without FCS. Every 24 hours the medium was changed. Forty-eight hours after the treatment cells were harvested for mRNA and protein analysis.

3.7.4. Treatment of A549 cells with panobinostat in different cell culture media

Two hundred thousand A549 cells per well were plated into six well plates in DMEM/F12 complete. Twenty-four hours after plating cells were washed twice with PBS to remove the medium residues. The cells were incubated with panobinostat or carrier (DMSO) under different glucose conditions in the absence or presence of FCS. Panobinostat (LBH589) was dissolved in DMSO (1 mM stock solution aliquots, stored at -20°C). After 48 hours of incubation cells were washed twice with PBS and collected for RNA or protein isolation.

3.7.5. LMK235 treatment of A549 cells

LMK235 is a specific inhibitor of human HDAC4 and 5 which inhibit the HDACs in a low nanomolar range (Hansen et al., 2014).

Two hundred thousand A549 cells per well were plated into six well plates in DMEM/F12 complete or in media with 10 mM glucose and 10% FCS. After 24 h cells were washed twice with PBS. Treatment with LMK235 (N-[[6-(Hydroxyamino)-6-oxohexyl]oxy]-3,5-dimethylbenzamidewas) or carrier (DMSO) was performed in starvation and non-starvation media. LMK235 was dissolved in DMSO (100 mM stock solution aliquots, stored at -20°C). After 48 hours the cells were collected for RNA or protein isolation.

3.7.6. HDAC3 inhibitor RGFP966

RGFP966 is a HDAC3 selective inhibitor with an IC50 of 0.08 µM. It does not inhibit other HDACs up to a concentration of 15 µM (Malvaez et al., 2013; Wells et al., 2013). In cutaneous T cell lymphoma RGFP966 leads to a lower cell growth (Wells et al., 2013).

Two hundred thousand cells were cultured in DMEM/F12 complete for 24 hours. On the second day cells were washed twice with PBS and incubated in starvation or non-starvation media with different RGFP966 concentrations.

A549 cells were collected after 24 or 48 hours to analyze the protein and mRNA amount.

3.7.7. Down-regulation of HDAC1, 2, 3, 4, 5 or 6 with siRNA

One hundred thousand A549 cells were cultured for 24 h in DMEM/F12 complete. Then transfection with the Jet Prime® kit was performed according to the manufacturer's instructions with a final siRNA concentration of 40 nM or 80 nM. On the next day medium was changed and fresh DMEM/F12 complete was given to the cells in six-well plates. After 48 h in DMEM/F12 complete the cells were cultured 48 h in starvation or non-starvation media. Every 24 h the medium was replaced, 6 days later cells were collected for RNA or protein isolation.

For the silencing tests cells were treated as described above but were collected 24 or 48 hours after the transfection.

3.7.8. Fluorescent-activating cell scanning analyses (FACS)

Caspase 3 is important for apoptosis; this was shown in caspase-3-deficient mice (Kuida et al., 1996). We used the CellEvent™ Caspase-3/7 Green Detection Reagent to analyze the activation of apoptosis after panobinostat treatment. The four amino acid peptide DEVD is a recognition side of caspase 3 and 7. DEVD is conjugated with a fluorescent substrate and if a caspase cleave the DEVD peptide the fluorescent can be measured (Garcia-Calvo et al., 1999).

Two hundred thousand cells were plated into 6-well plates in DMEM/F12 complete. After 24 hours cells were treated with different panobinostat concentrations and DMSO as a vehicle control. After 48 hours apoptosis was measured with the CellEvent™ Caspase-3/7 Green Detection Reagent assay. The CellEvent solution was diluted 1:125 in DMEM/F12 complete. The supernatant was collected and the well was washed with 1 ml PBS which was also collected. Five-hundred µl trypsin were added and tyrpsinized cells were collected. To stop the trypsin reaction DMEM/F12 complete was added to the cells. Wells were washed with PBS. Medium and PBS were collected. About 500,000 cells were used for analysis. Samples were centrifuged at 400 g for 5 minutes, resuspended in PBS and centrifuged again for 5 minutes at 400 g. The pellet was dissolved in 62.5 µl CellEvent solution and incubated for 45 minutes

at 37°C in the dark. After that time 250 µl PBS was pipetted to the cells. Samples were analyzed using the CytoFLEX (Beckman Coulter, Barea, California, USA). The fluorescence emission at around 530 nm ("Thermo Fisher," 2016) was detected by using a standard FITC filter set (Figure 8).

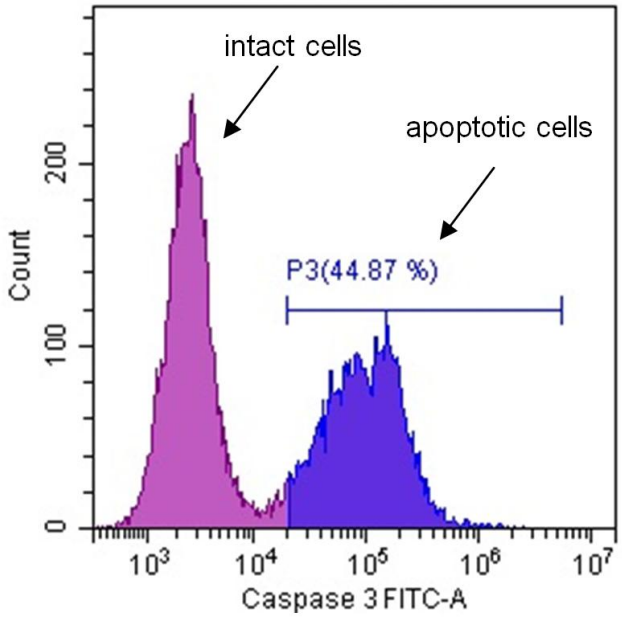

Figure 8: Apoptosis analyses by FACS. Two hundred thousand A549 cells per well were plated in DMEM/F12 complete. Cells were treated with panobinostat for 48 hours. The apoptosis was measured with the CellEvent™ Caspase-3/7 Green Detection Reagent assay.

3.8. SDS-PAGE gel electrophoresis and Western blot

SDS-PAGE gel electrophoresis was performed to separate cell proteins according to their size. Subsequently a Western blot was used to detect the amount of specific protein in the cell lysates.

3.8.1. Sample preparation

Cells were washed twice with PBS and only adherent cells were collected. Then cells were scraped on ice in RIPA buffer with protease- and phosphatase-inhibitors. Cell lysates were homogenized using a sonicator (Ultraschall-Desintegrator UP50H ROTH, Carl Roth GMbH+Co.KG Karlsruhe, Deutschland) at amplitude of 80 and at cycle 1. Each sample was sonicated twice for two seconds. Insoluble material was removed by centrifugation at 13,000 rpm for 10 minutes at 4°C. The supernatants were collected and stored at -20 °C.

3.8.2. Determination of the protein concentration

Protein concentration was measured with the BCA (bicinchononic acid) Protein Assay Kit in duplicates. Twenty-five µl diluted sample (1:5) and 200 µl BCA solution were mixed. Linear calibration curve was made using a serial dilution of a 2 mg/ml BSA stock. Absorption was measured in 96 well plates using the Spectramax Plus 384 (Molecular Devices, Orleans Drive Sunnyvale, CA).

3.8.3. SDS-PAGE gel electrophoresis

Samples were diluted with RIPA buffer as appropriate, mixed with 5x Laemmli buffer and heated at 95°C for 10 minutes on the Thermomixer comfort (Eppendorf, Hamburg, Germany). Twenty µg total proteins were loaded per lane on the gel. Electrophoresis was performed at 160 V or 180 V in electrophoresis running buffer. The Precision Plus Protein™ Dual Color Standard (BioRad Industries, Hercules CA) was used for all experiments.

3.8.4. Western blot

Separated proteins were transferred onto a polyvinylidene difluoride (PVDF) membrane or on a nitrocellulose membrane to proceed with protein detection. The transfer was achieved at 400 mA for 1:30 h to 1:45 h, dependent on the protein size. To control the transfer efficiency, proteins on the membrane were stained with Ponceau-S-red. The membrane was destained with water and blocked for one hour in 5% milk TBS-T (MTBST) solution at room temperature to inhibit unspecific antibody binding. The membrane was incubated with the antibody solution overnight at 4°C. On the next day three washing steps for 10 minutes each with TBS-T followed. The membrane was incubated for one hour with the secondary antibody in TBS-T. Afterwards the membrane was washed three times for 15 minutes with TBS-T to remove antibody which did not bind. Thereafter the signal was detected with the Amersham ECL Prime Western Blotting Detection Reagent or with the Super Signal WesternPico Chemiluminescent Substrate according to the manufacturer's instructions.

The Amersham Hyperfilm ECL high performance chemiluminescence film and the T-MAT, G/RA film were used for the detection. The film was developed in the darkroom with the Curix 60 (Agfa, Healthcare). Alternatively chemiluminiscence was visualized with the ChemiDoc Touch Imager (BioRad

Industries, Hercules CA).

To reuse membranes for other antibodies stripping was performed. The membrane was washed for 5 minutes with TBST, incubated for 15 minutes in Restore PLUS Western Blot stripping buffer, washed twice for 5 minutes with PBS and once for 5 minutes with TBST. Then the blocking step in 5% MTBST was repeated.

3.9. Reverse transcription and quantitative real-time polymerase chain reaction

The isolated mRNA from the cells was reversely transcribed to cDNA and a quantitative real-time polymerase chain reaction (qPCR) was performed to detect the specific mRNA amount from the cell.

3.9.1. RNA isolation and measurement

The total RNA (further referred as RNA) was isolated with the peqGOLD® Total RNA Kit according to the manufacturer's instructions. The additional DNAse digestion was only necessary for RNA used as a template for HDAC qPCR. RNA was finally eluted with 40 µl H_2O. After isolation the RNA amount was measured with Nano Drop (Thermo Scientific, Fremont, USA).

3.9.2. Reverse transcription

The reverse transcription was performed using the iScript™ cDNA Synthesis Kit according to the manufacturer's instructions. The kit uses the reverse transcriptase RNase H^+ and a mixture of oligonucleotides and random hexameric primers. Depending on the RNA amount 250 to 500 ng total RNA were reversely transcribed in a total volume of 20 µl. The reverse transcription program was performed in the My Cycler™ thermal cycler (Bio-Rad). The conditions for the reverse transcription were: 25°C for 5 minutes, 42°C for 30 minutes and 85°C for 5 minutes.

3.9.3. Quantitative real-time polymerase chain reaction

Quantitative real-time PCR was performed using the LightCycler 480 (Roche, Vienna, Austria) and the QuantiFast SYBR PCR kit. For qPCR the cDNA was diluted 1:4 or 1:8, dependent on the cDNA concentration and the used primer

pair. Two and a half µl syber green master mix and 0.5 µl primer mix were used in 4 µl reactions. Melting curve analysis was performed to confirm the amplification of a specific PCR product. Reactions were performed in duplicates. Beta-actin and beta-2 microglobulin served as reference genes. Mean Ct values calculated for beta-actin and beta-2 microglobulin (Ct_{Ref}) were stable across all the different panobinostat treatments and used as reference values. ΔCt was calculated by subtracting mean Ct values of PCK2 from Ct_{Ref}. For samples without panobinostat treatment beta-actin was used for the normalization. ΔCt was calculated by subtracting mean Ct values of PCK2 from the mean Ct value of beta-actin.

The temperature profile was as follows: pre-incubation 95°C 10 minutes, amplification: 95°C 10 seconds, 60°C 10 seconds, 72°C 20 seconds, 45 cycles were made. Thereafter melting curves were generated at 95°C 10 seconds, 55°C 1 minute, 95°C continuous.

3.9.4. Primer test

The cDNA of untreated A549 cells was diluted 1:4, 1:8, 1:16 and 1:256. Also a RT minus control (without reverse transcriptase in the cDNA synthesis) and a NTC (no template control, qPCR with aqua dest. instead of cDNA) were made. The samples were analyzed on a 3% agarose gel. Electrophoresis was performed at 100 V and the gel was analyzed by using the Gel Doc™ XR+ System (BioRad Industries, Hercules CA).

3.10. Phase contract microscopy

Cells were visualized and photographed with the Olympus Ckx31 Inverse Microscope (Olympus, Vienna, Austria) and Cell^F software.

3.11. Densitometric analyses of Western blots

Western blot bands were quantified with the Image Lab 5.2 (BioRad Industries, Hercules, CA).

3.12. Statistical analysis

Calculations and graphs were made with Excel 2010. Group comparisons were performed using Student´s t-test. One group Student´s t-tests were performed with the SPSS software package, version 21 (Chicago, IL). Results from at least

three independent experiments were used for statistical analysis. P-values smaller than 0.05 were considered significant. .* $p < 0.05$; ** $p < 0.01$; *** $p < 0.001$. All calculations were made in comparison to DMSO.

4. Results

4.1. Acetylation of histone 3 and histone 4 was increased after panobinostat treatment

It has been shown that HDACs are necessary for the expression of gluconeogenesis genes in the liver (Mihaylova et al., 2011). We wanted to investigate if PCK2, a gluconeogenesis enzyme which is important under starvation conditions in lung cancer cells (Leithner et al., 2015), is regulated by HDACs. Preliminary results showed effects of panobinostat, a pan-HDAC inhibitor, on PCK2 mRNA levels in lung cancer cells (Leithner K., unpublished data). As a proof of concept we analyzed the effect of panobinostat on the acetylation status of histones 3 and 4 in A549 lung cancer cell lines. Cells were treated with increasing panobinostat concentrations under different medium conditions. Higher panobinostat concentrations correlated with a higher acetylation level of histone 3 and 4. Similar effects were also described in previous studies (Fischer et al., 2015; Greve et al., 2015). Figure 9 shows concentration-dependent acetylation effects of panobinostat which were especially prominent under starvation conditions (0.2 mM glucose and no feal calf serum).

A

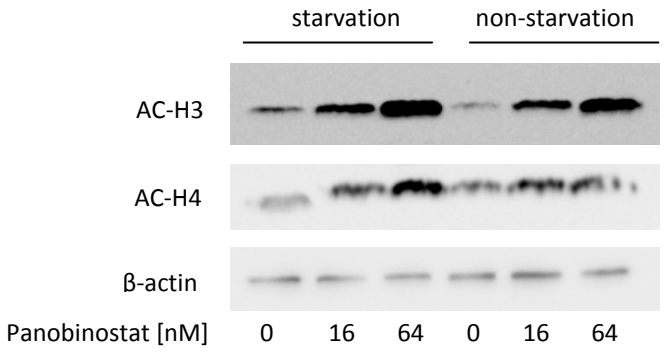

B

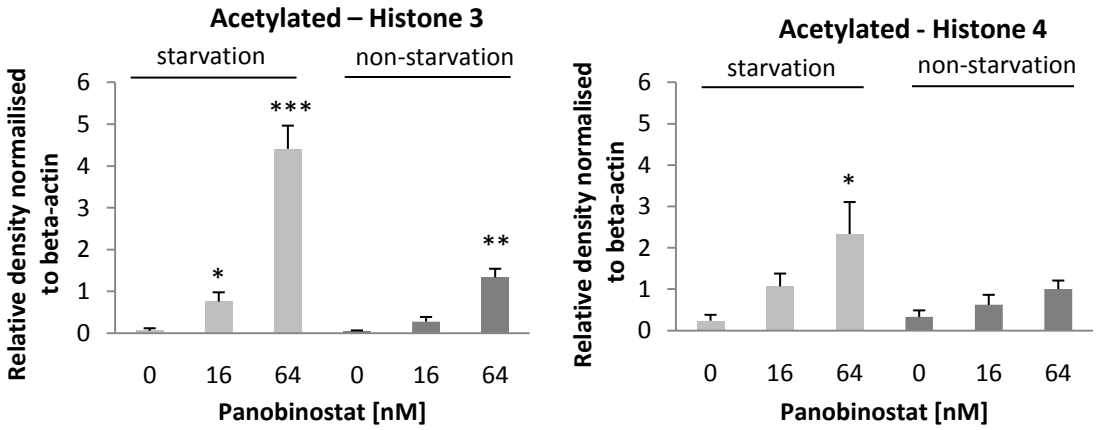

Figure 9: Acetylation level of histone 3 and 4 after panobinostat treatment in A549 cells. A549 cells were incubated with different panobinostat concentrations for 48 hours. After that time cells were harvested and the cell lysate was prepared. Acetylation of histones was verified by immunoblot. DMSO was used as a vehicle control (0 nM panobinostat). (A) Representative Western blots are shown. (B) Blots from three independent experiments were analyzed by densitometry. The statistics were made with the Student´sT-test.* $p < 0.05$; ** $p < 0.01$; *** $p < 0.001$. All calculations were made in comparison to DMSO. Results are shown as a mean +/- SEM from three independent experiments. AC, acetylated; H, histone

4.2. PCK2 expression did not change after panobinostat treatment in DMEM/F12 complete medium

Panobinostat treatment showed the expected changes of histone acetylation. Next, we treated A549 cells in DMEM/F12 complete medium with panobinostat and analyzed the protein amount of PCK2. Panobinostat concentrations in a low nanomolar range were used to treat the A549 cells (0, 8, 16, 32, 64, 128 and 256 nM) (Figure 10). Previous studies from our group used the same panobinostat concentration for A549 cells (Fischer et al., 2015). The PCK2 amount did not change after 48 hours panobinostat treatment in DMEM/F12

complete (Figure 10). However, the cells were very sensitive to highest panobinostat concentrations (128 and 256 nm) and the total protein amount was much lower than in other samples.

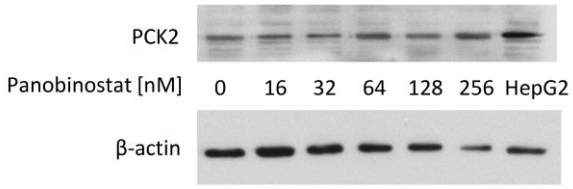

Figure 10: PCK2 expression in A549 cells under different panobinostat concentrations in DMEM/F12 complete medium. Cells were first incubated in DMEM/F12 complete medium for 24 hours. Samples were collected 48 hours after the initiation of panobinostat treatment (0, 8, 16, 32, 64, 128 and 256 nM). The amount of PCK2 was analyzed with Western blot. HepG2 cell-lysate was used as a positive control for the antibody. Beta-actin was used as a loading control. A representative Western blot is shown. DMSO was used as a vehicle control at the same dilution as for the highest panobinostat concentration. Representative immunoblots from two experiments are shown.

4.3. FACS analyses after panobinostat treatment showed an increase of apoptotic cells at low nanomolar concentrations

Higher panobinostat concentrations (128 and 256 nM) visibly induced cell death in A549 cells. As described previously in other cell lines, panobinostat can activate the apoptotic caspase pathway (Crisanti et al., 2013; Lemoine et al., 2012). When we measured the apoptotic effects of panobinostat by a caspase 3 assay with fluorescence activated cell sorting (FACS), we found that the number of apoptotic cells clearly increased at panobinostat concentrations higher than 64 nM (Figure 11 B). Therefore, for further experiments we decided to treat our cells with a maximal concentration of 64 nM in order to avoid possible secondary effects of apoptosis on PCK2 expression. Figure 11 A shows the FACS analyses of apoptotic cells after treatment with different panobinostat concentrations. Figure 11 B shows the percentage of apoptotic cells from three independent experiments.

A

negative control

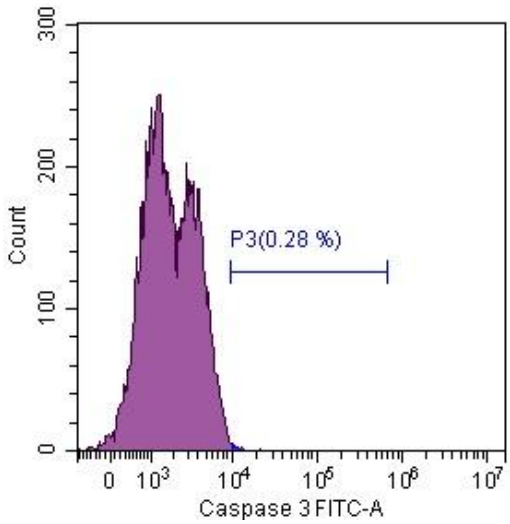

DMSO

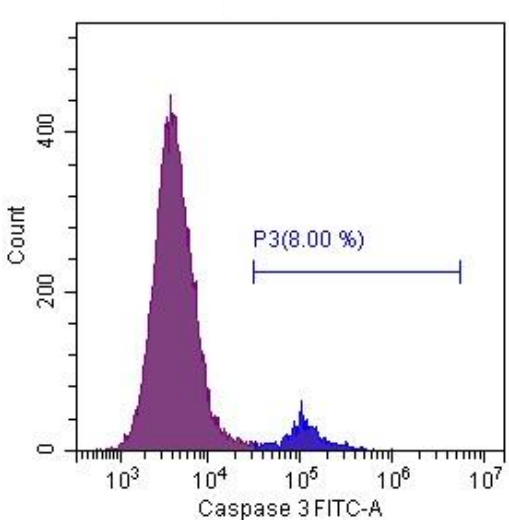

64 [nM] panobinostat

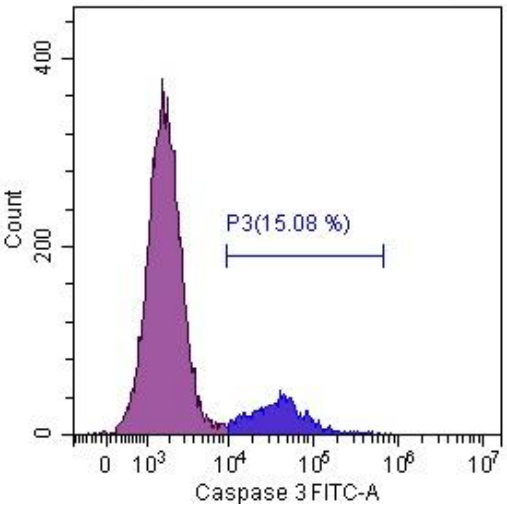

256 [nM] panobinostat

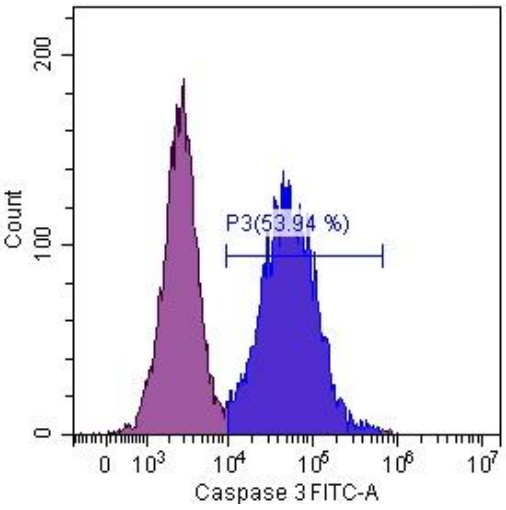

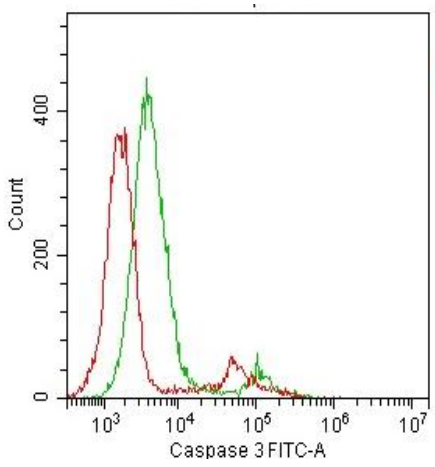

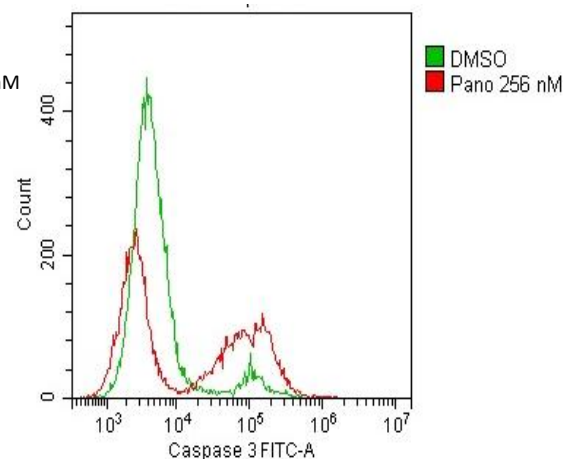

B

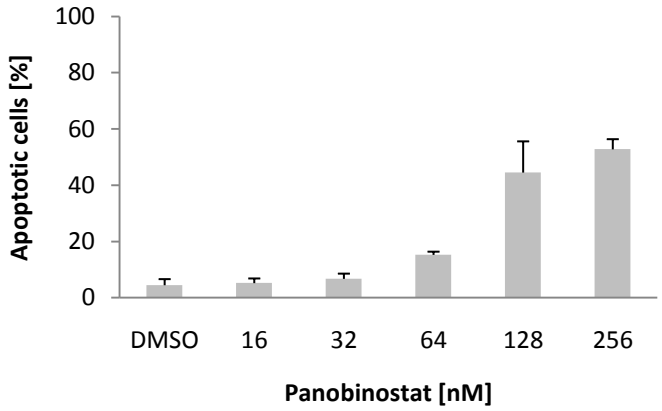

Figure 11: FACS analyses after panobinostat treatment. A549 cells were treated for 48 hours with different panobinostat concentrations and collected for the caspase assay. Approximately 500,000 cells were analyzed by FACS. DMSO was used as a vehicle control. Representative graphics from three independent experiments are shown in (A). The negative control shows cells which have not been incubated with the caspase 3-cleavable peptide (Cell Event solution). (B) Mean percentage of apoptotic cells from three independent experiments. Results are shown as a mean +/- SEM.

4.4. Panobinostat treatment leads to a lower cell density in A549 cells

PCK2 is a gluconeogenesis enzyme with increased expression under low glucose conditions in lung cancer cells (Leithner et al., 2015). In this project we aimed to analyze the effects of HDAC inhibition on PCK2 under starvation and non-starvation conditions. Therefore, we addressed the question, which concentrations of panobinostat do not lead to massive cell death, also under glucose deprivation. We analyzed A549 cell morphology under a low (0.2 mM), intermediate (1 mM) and high (10 mM) concentration of glucose in the presence or absence of 10% dialyzed FCS. At the highest glucose conditions (10 mM) the cell density was higher than under starvation conditions (0.2 mM glucose and 0% FCS). In medium with FCS the cell density was higher compared with medium without FCS. Panobinostat reduced the cell density, those effects being most prominent in starvation medium. At highest panobinostat concentration (64 nM) there were also more detached cells then at the DMSO control, especially under starvation conditions. However the majority of cells still survived at concentrations of 64 nM panobinostat, under starvation and non-starvation

conditions. Thus, we used panobinostat concentrations up to 64 nM for our experiments. The effects of panobinostat on the cell morphology under different media conditions were documented 48 hours after panobinostat treatment (Figure 12).

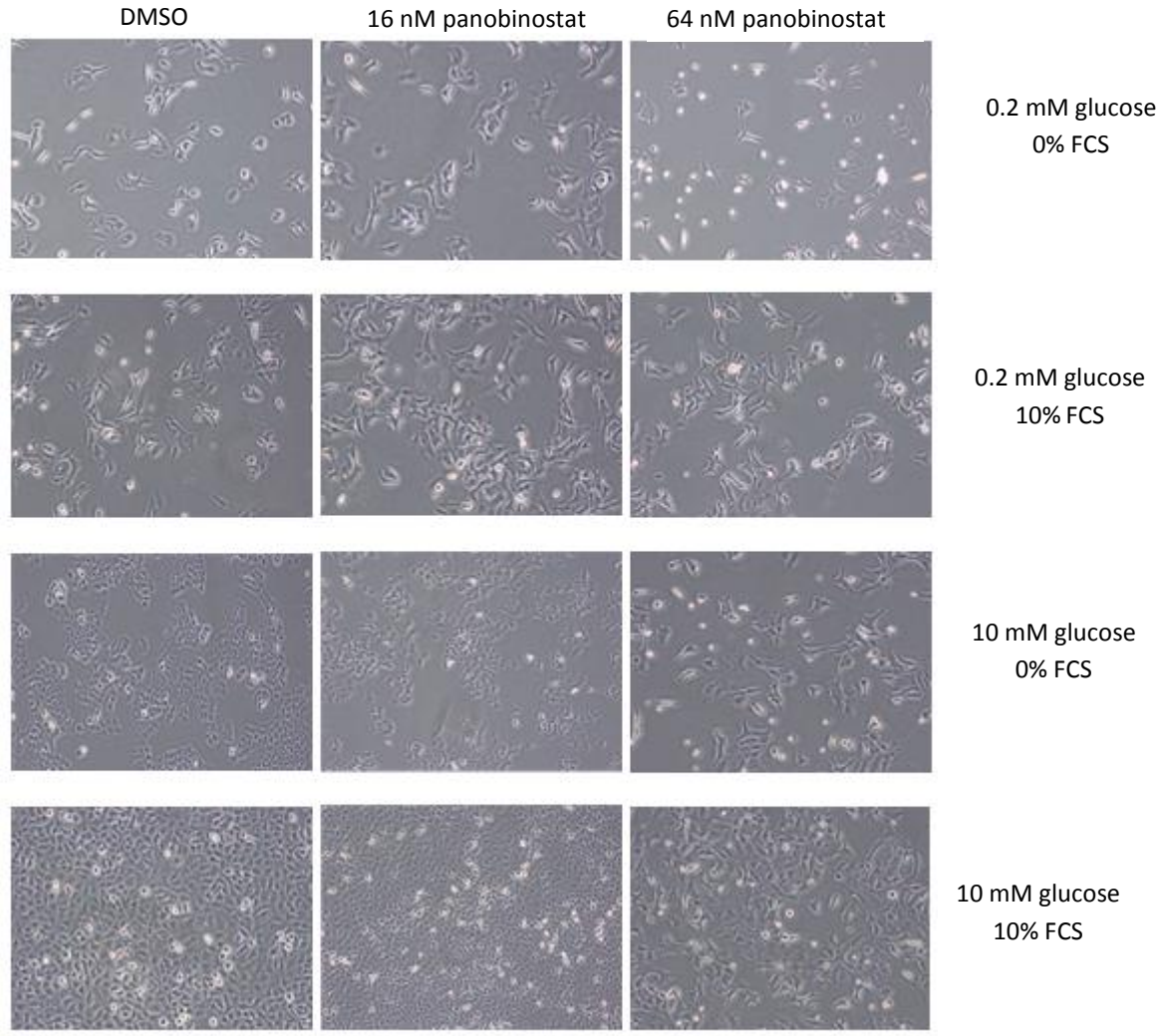

Figure 12: Phase contrast microscopy images of A549 cells 48 hours after panobinostat treatment under different media conditions. Cells were seeded into a six well plate in DMEM/F12 complete medium and incubated for 24 hours. Thereafter cells were treated with panobinostat in media containing 0.2, 1 and 10 mM glucose, with or without 10% FCS. These six conditions were combined with panobinostat concentrations of 0, 8, 16, 32, and 64 nM. The cells were incubated for 48 hours in these media. Representative images are shown. FCS, fetal calf serum. n = 3

4.5. Primer testing and reference gene analyses

Primer testing was necessary in order to prove the specificity of the qPCR. We tested different template dilutions and controls. CDNA from A549 cells served as a template. Controls without template (non-template control) and RT-controls (without reverse transcriptase during the cDNA synthesis) were included. The differences between the Ct values from the sample and the Ct values of the RT- control were small and there were no clear bands on the agarose gel. This might have indicated the amplification of genomic DNA by this pair of primers. Therefore we introduced the DNase digestion in our RNA isolation protocol, resulting in a close to negative result in the RT- control. Based on this we did the DNase digestion for all samples analyzed with HDAC primers. For PCK2 primer DNase digestion was not necessary to get good Ct values for the sample and also for the RT- control.

For qPCR experiments it is important to identify one or more suitable reference gene to get reliable results. Ct values from reference gene and target genes should be in a similar range and the reference gene(s) should be stably expressed (Kozera et al., 2013).

We tested two reference genes but their Ct values were not fully stable after panobinostat treatment. Beta-actin showed higher Ct values at higher panobinostat concentrations (Figure 13 A). Beta-2 microglobulin was more stable but also not over all conditions (Figure 13 B). However, the mean values of these two genes (Ct_{Ref}) were more constant and were used for further analyses of panobinostat-treated cells (Figure 13 C). In all other experiments beta-actin showed a stable expression and was used as reference gene.

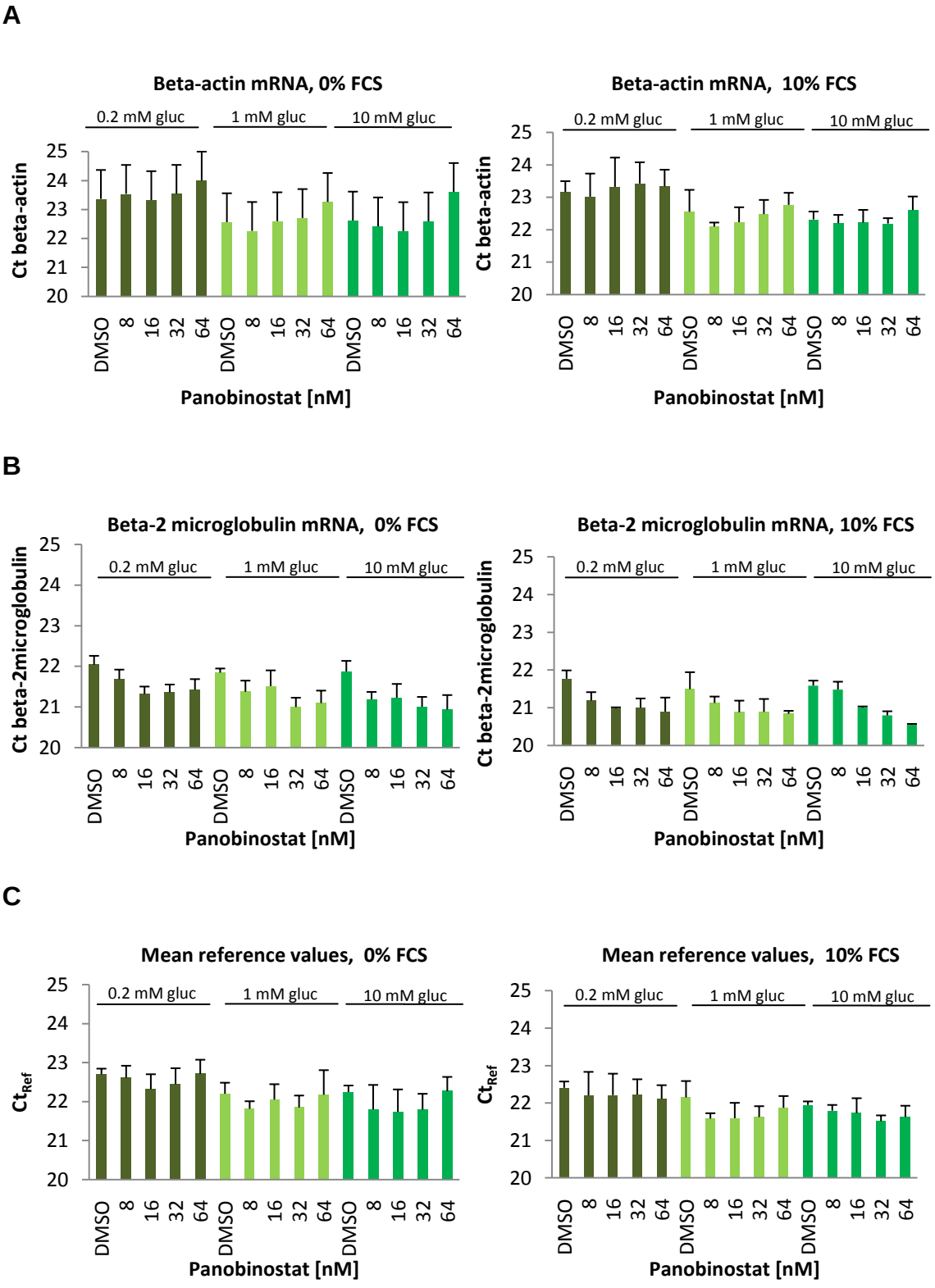

Figure 13: Ct values of reference genes under different medium conditions. A549 cells were treated with panobinostat and cultivated using different glucose and FCS concentrations. After 48 hours RNA was isolated and reverse transcribed into cDNA. Expression levels of specific mRNAs were analyzed using qPCR. Expression levels of beta-actin (A) and beta-2 microglobulin (B) were not completely stabile. The mean value from beta-actin and beta-2 micoglobulin was calculated (Ct_{Ref}), being more stable over all conditions (C). Results are shown as mean +/- SEM from three independent experiments. FCS, fetal calf serum; gluc, glucose.

4.6. Panobinostat reduced mRNA and protein levels of PCK2

By using the Ct_{Ref} values for normalization we analyze the PCK2 expression after panobinostat treatment under different media conditions. QPCR data showed a reduction of the PCK2 expression in cells treated with increasing panobinostat concentration (Figure 14 A). Glucose and FCS concentration affected PCK2 expression on mRNA level (Figure 14 A).

In addition, the PCK2 protein amount was evaluated by Western blot after panobinostat treatment in different media. At the highest panobinostat concentration (64 nM), panobinostat inhibited PCK2 expression significantly under starvation conditions. In medium without FCS the effects of panobinostat on PCK2 expression were higher than in medium with FCS (Figure 14 C).

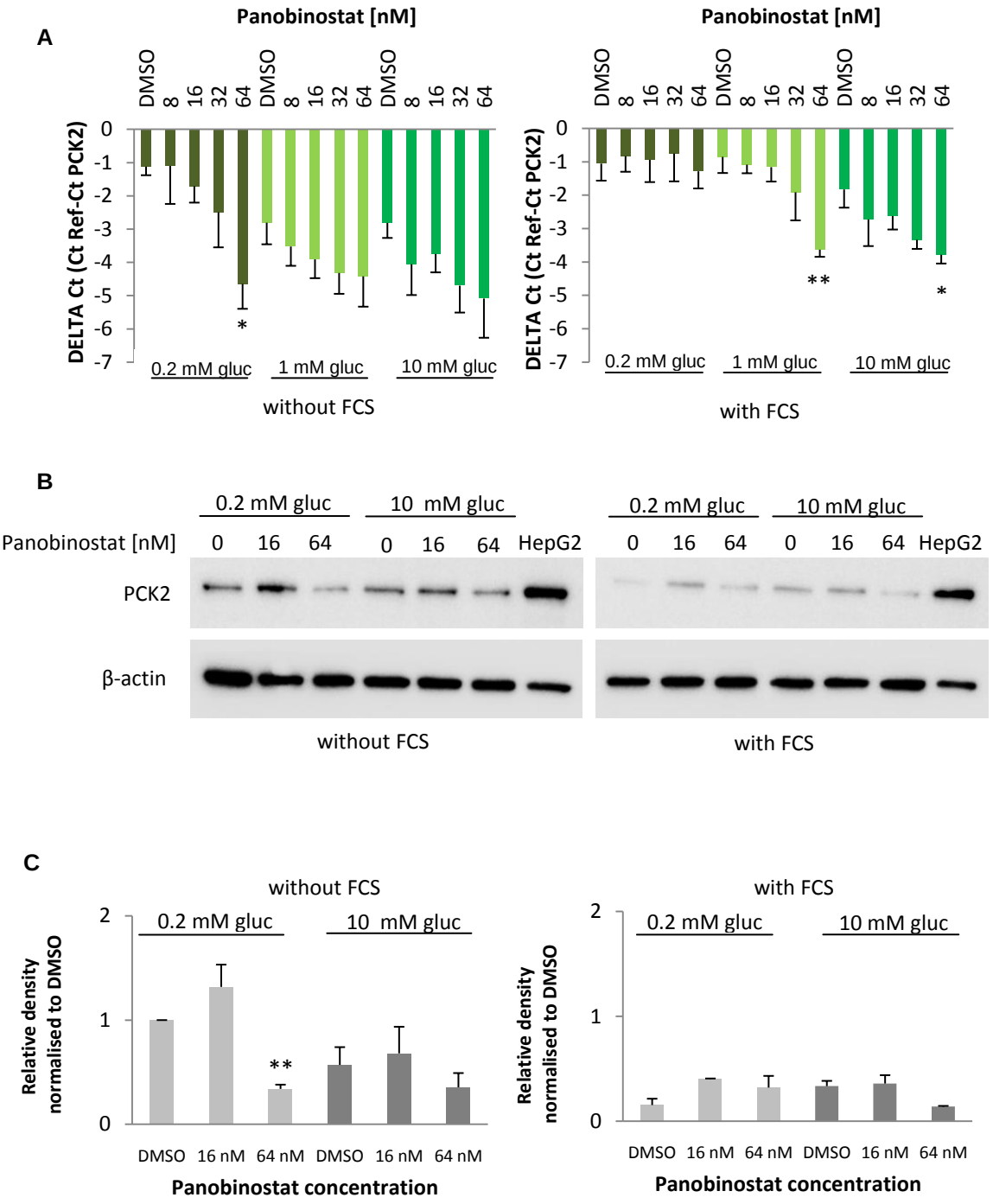

Figure 14: PCK2 expression in A549 cell cultivated under different panobinostat, glucose and FCS concentrations. Samples were collected after treatment with panobinostat for 48 hours in media containing different concentrations of glucose, with or without dialyzed FCS. (A) The mRNA amount was measured with a qPCR. (B) Representative immunoblots are shown. (C) Relative density of PCK2 signals normalized to DMSO. The diagram in the left panel shows different conditions without FCS. The diagram in the right panel shows results from experiments with FCS. The statistics were made with a t-test.* $p < 0.05$; ** $p < 0.01$; *** $p < 0.001$. All values were compared to DMSO control. Results are shown as mean +/- SEM from three independent experiments. FCS, fetal calf serum; gluc, glucose.

4.7. Silencing of different HDACs

Panobinostat is an inhibitor of class I and II HDACs (Laubach et al., 2015; Bailey et al., 2015). Our results indicate that panobinostat influences the PCK2 mRNA and protein amount. Therefore we silenced different HDACs to learn more about their regulatory function on PCK2.

4.7.1. Silencing of different HDACs with siRNA showed a significant decrease of HDAC expression

First we did some pilot silencing experiments for HDAC1, 2, 3, 4, 5 and 6 to determine the time point at which at least 70% knockdown can be reached, in comparison to cells which were transfected with control siRNA. We used a pool of 4 specific siRNA sequences for each particular HDAC. For further analyses the silencing effects in cells transfected with HDAC specific siRNA were compared to the effects in cells transfected with the control siRNA. After 48 hours all HDAC siRNAs showed significant silencing effects. The results from the silencing of HDAC1 (A), HDAC2 (B), HDAC3 (C), HDAC4 (D), HDAC5 (E) and HDAC6 (F) are shown in Figure 15. HDAC1 and HDAC2 silencing was only tested after 48 hours. A summary of knockdown effects for different HDACs is shown in table 10. The siRNA concentration used in all experiments was 40 nM. Protein and mRNA amount of HDACs was analyzed by Western blotting and qPCR (Figure 15). Detailed analyses showed that the HDAC6 antibody was not specific, therefore only mRNA amount for the HDAC6 was analyzed.

A

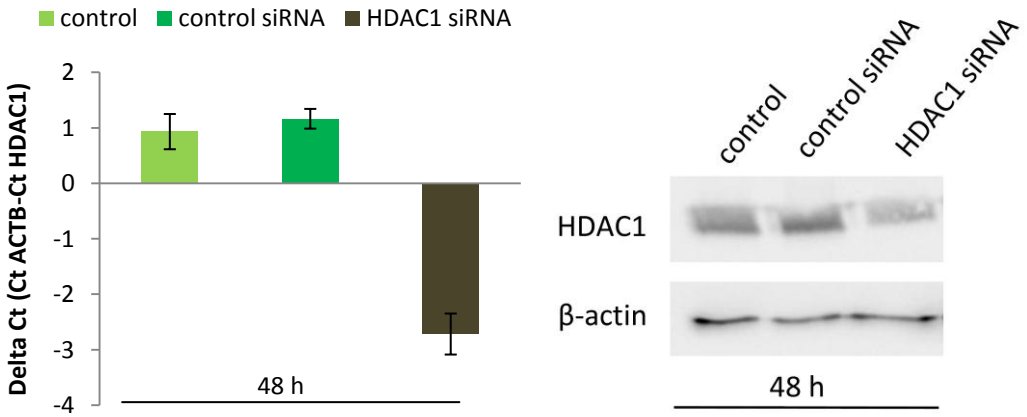

B

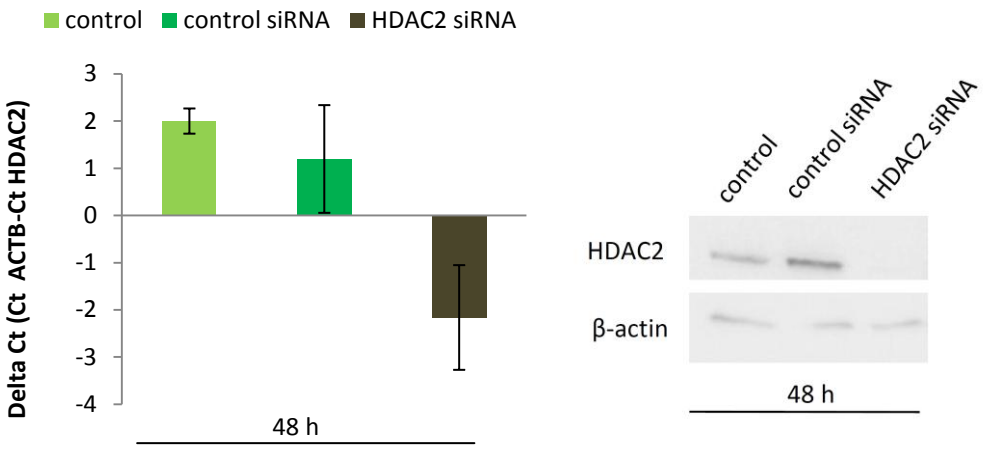
control
control siRNA
HDAC2 siRNA
Delta Ct (Ct ACTB-Ct HDAC2)
3
2
1
0
-1
-2
-3
-4
48 h
control
control siRNA
HDAC2 siRNA
HDAC2
β-actin
48 h

C

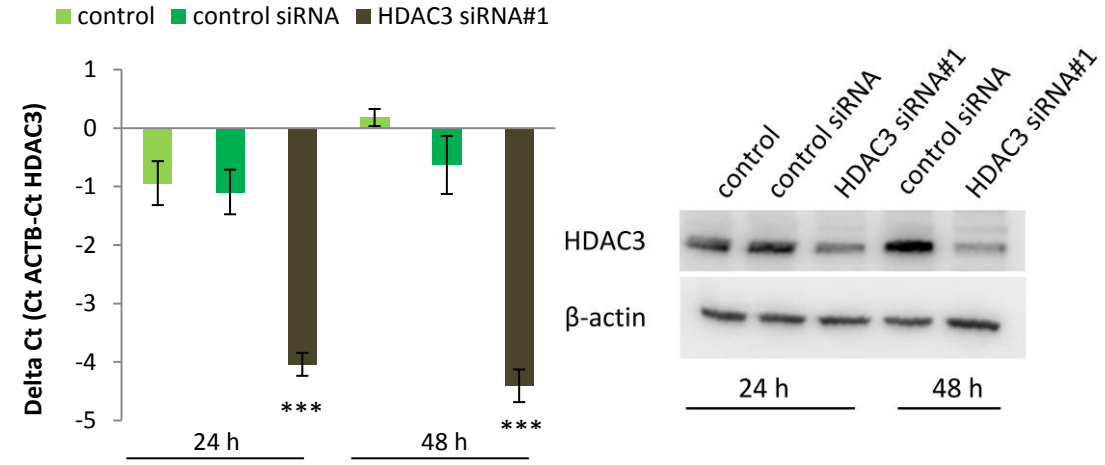
control
control siRNA
HDAC3 siRNA#1
Delta Ct (Ct ACTB-Ct HDAC3)
1
0
-1
-2
-3
-4
-5
***
***
24 h
48 h
control
control siRNA
HDAC3 siRNA#1
control siRNA
HDAC3 siRNA#1
HDAC3
β-actin
24 h
48 h

D

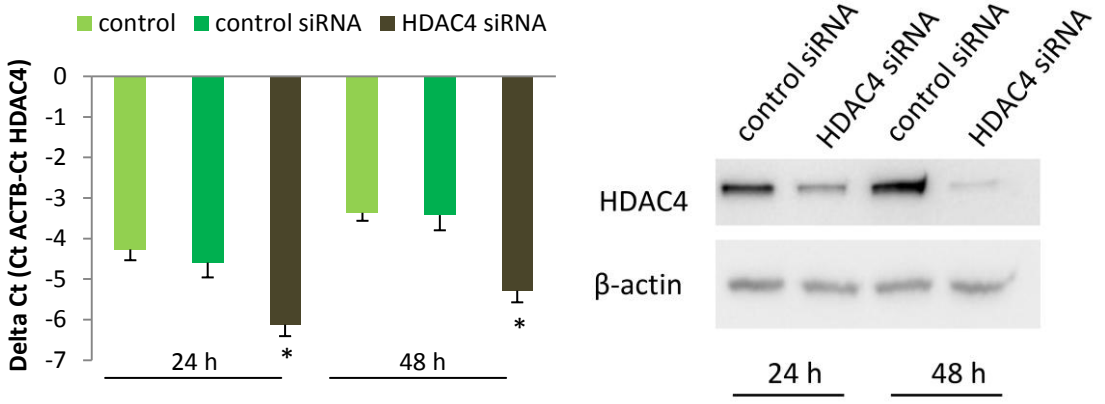
control
control siRNA
HDAC4 siRNA
Delta Ct (Ct ACTB-Ct HDAC4)
0
-1
-2
-3
-4
-5
-6
-7
*
*
24 h
48 h
control siRNA
HDAC4 siRNA
control siRNA
HDAC4 siRNA
HDAC4
β-actin
24 h
48 h

E

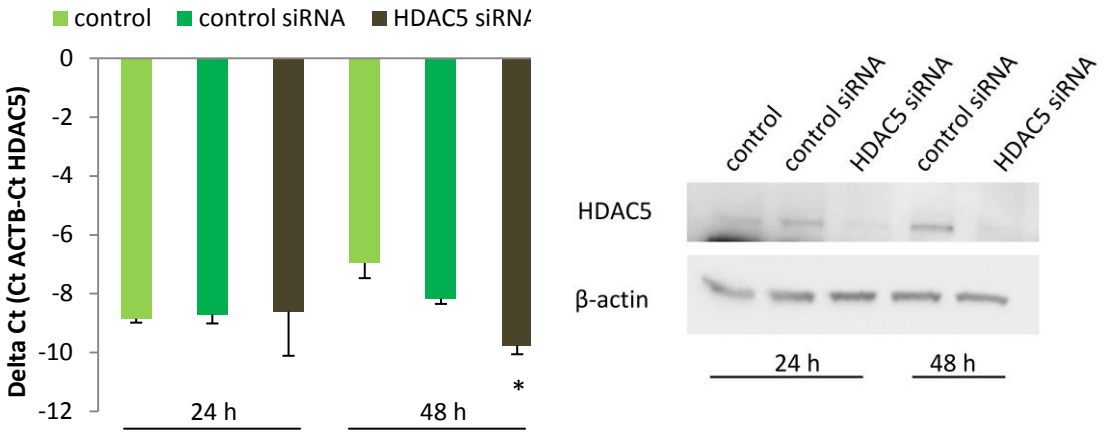

F

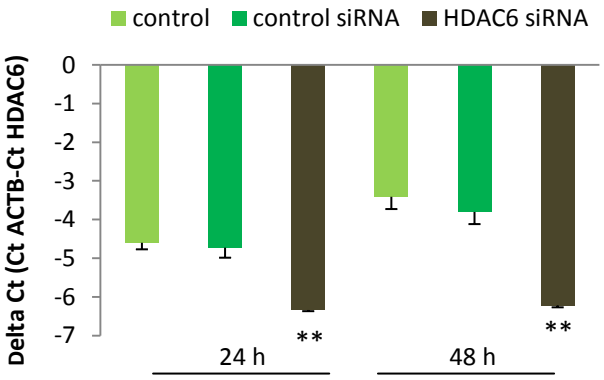

Figure 15: Effects of HDACs silencing after transfection for 24 and 48 hours. Cells were cultured 24 hours in DMEM/F12 complete and were then transfected with control siRNAs and HDAC siRNAs. Twenty four hours after transfection cells were collected for RNA and protein analyses or the medium was changed and cells were collected 48 hours after transfection. QPCR and Western blot results are shown for HDAC1 (A), HDAC2 (B), HDAC3 (C), HDAC4 (D) and HDAC5 silencing (E). For HDAC6 silencing only qPCR data are shown (F). Representative Western blots are shown. The statistics were made with a t-test.* $p < 0.05$; ** $p < 0.01$; *** $p < 0.001$. All samples were compared to DMSO control. Results are shown as mean +/- SEM from three independent experiments. Control, untransfected cells.

Table 10: Silencing effects on HDACs mRNA after 24 and 48 hours.

HDAC	24 hours [%]	48 hours [%]
HDAC3	87	94
HDAC4	65	73
HDAC5	0	77
HDAC6	67	81

4.7.2. HDACs silencing effects on PCK2 under starvation and non-starvation conditions

It was shown that PCK2 expression is higher under starvation conditions then under non-starvation conditions (Leithner et al., 2015). To evaluate the influence of specific HDACs on PCK2 expression we performed silencing experiments under starvation and non-starvation conditions. Previous experiments showed significant knockdown effects up to 90% after 48 hours. After that time the A549 cells were cultured in starvation and non-starvation medium for another 48 hours before analyzing the PCK2 expression.

A diagram summarizing the protocol of the silencing experiments under starvation and non-starvation conditions is shown in Figure 16. HDAC silencing showed significantly lower HDAC mRNA levels in all samples under starvation and non-starvation conditions compared to the control siRNA. There was no effect on PCK2 mRNA and protein amount after HDAC1 and HDAC2 silencing (Figures 17, 18). In contrast, down-regulation of HDAC3 expression did affect the PCK2 protein and mRNA expression (up to 90% PCK2 mRNA reduction) (Figure 19, Table 11). HDAC4 protein and mRNA amount showed a trend to a lower expression (Figure 20). HDAC5 and HDAC6 silencing showed no or only small effects under starvation conditions on the PCK2 protein and mRNA amount (Figures 21, 22). Table 11 summarizes the HDACs silencing effects on PCK2 mRNA and protein amount.

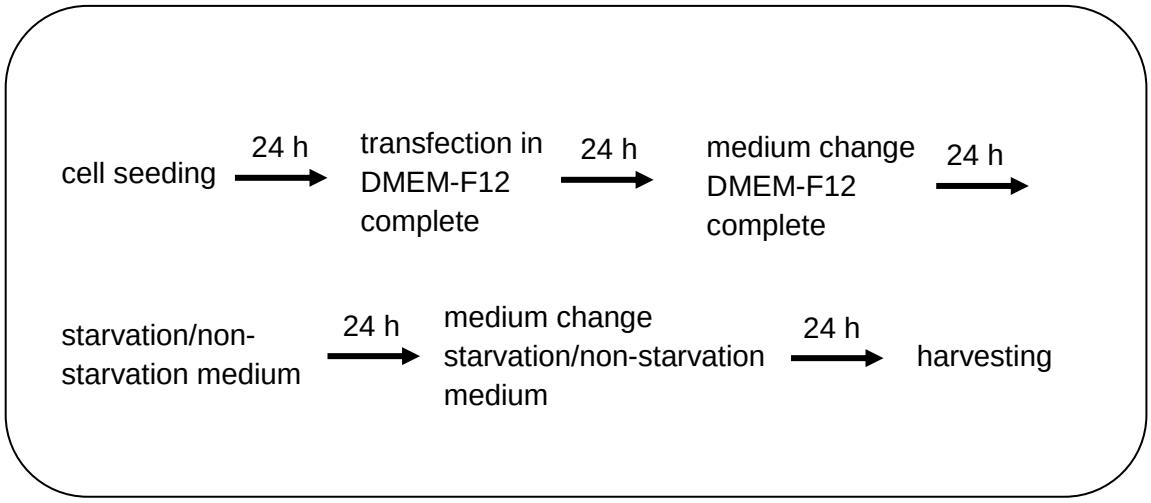

Figure 16: Cell treatment for transfection experiments.

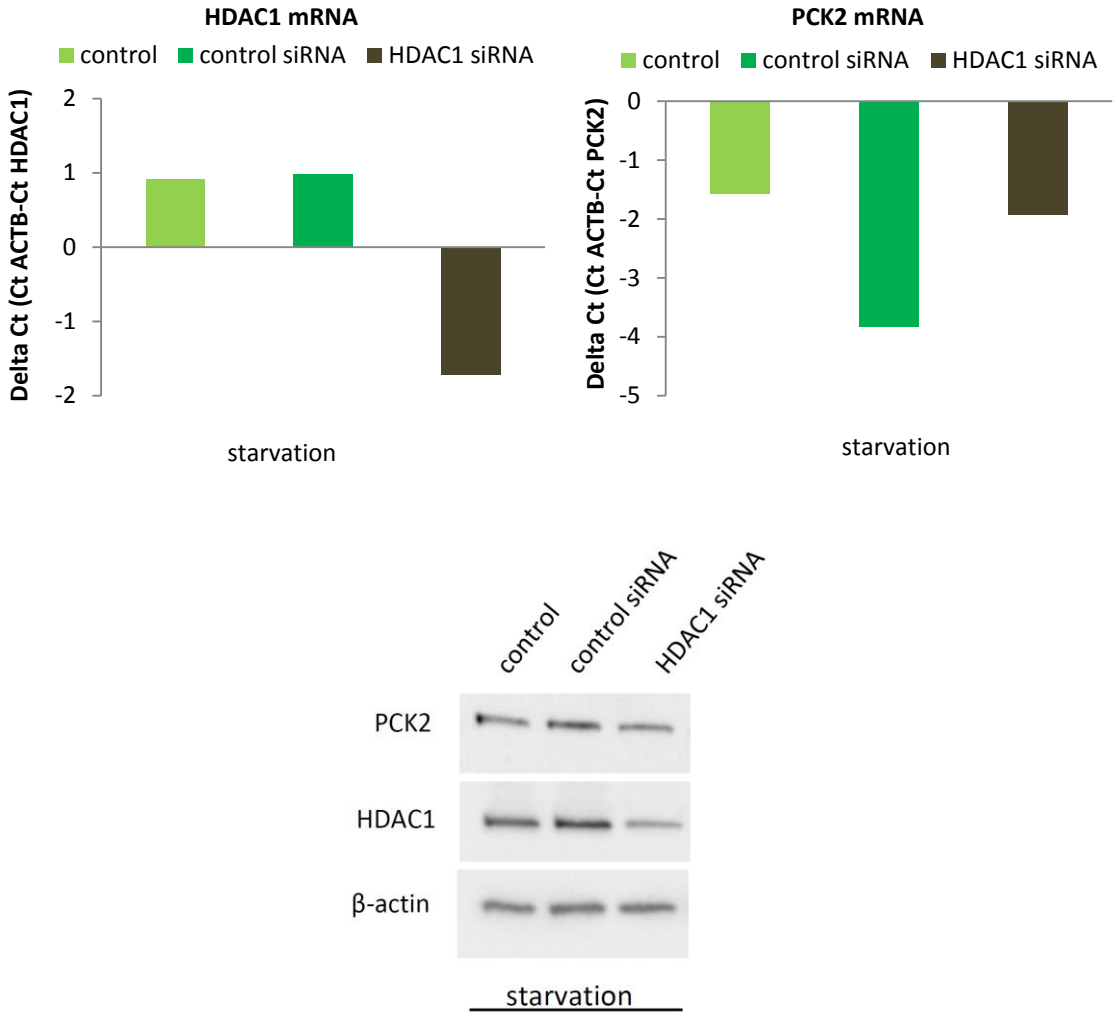

Figure 17: HDAC1 silencing under starvation conditions. A549 cells were cultivated 24 hours in DMEMF/12 complete. Cells were transfected with 40 nM control siRNA or HDAC1 siRNA. Twenty-four hours later fresh DMEM/F12 medium was given to the cells. On the next day cells were washed twice with PBS and cultured in starvation medium for 48 hours. Every 24 hours medium was changed. Cells were collected for qPCR and Western blot. Representative Western blots are shown. n=2; control, untransfected cells.

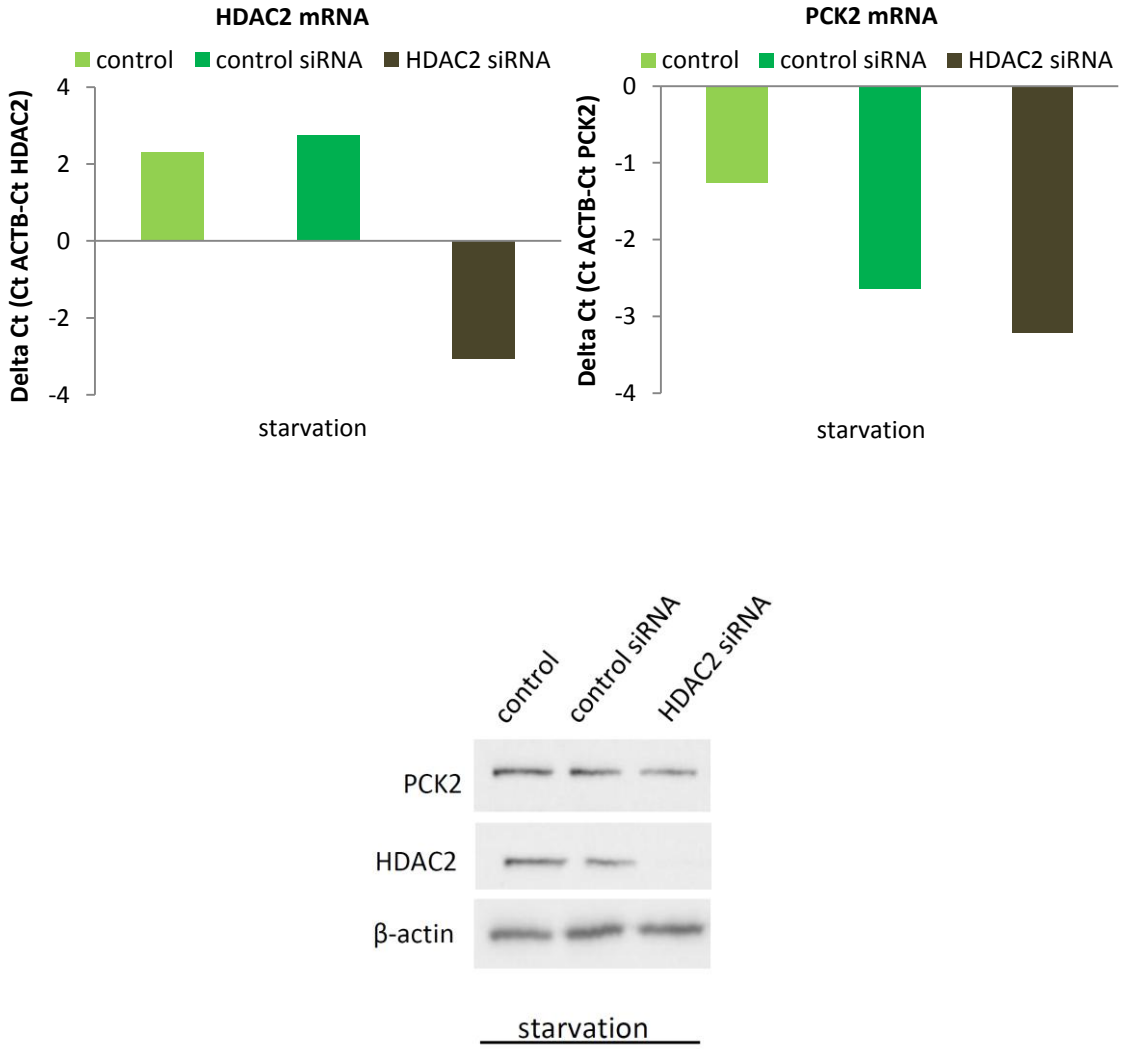

Figure 18: HDAC2 silencing under starvation conditions. Twenty-four hours after plating the cells in DMEM/F12 they were transfected with 40 nM control siRNA or HDAC2 siRNA. Another 24 hours later DMEM/F12 medium was given to the cells. On the next day cells were cultured in starvation medium for 48 hours. Every 24 hours medium was changed. Cells were collected for qPCR and Western blot. Representative Western blots are shown. n=2; control, untransfected cells.

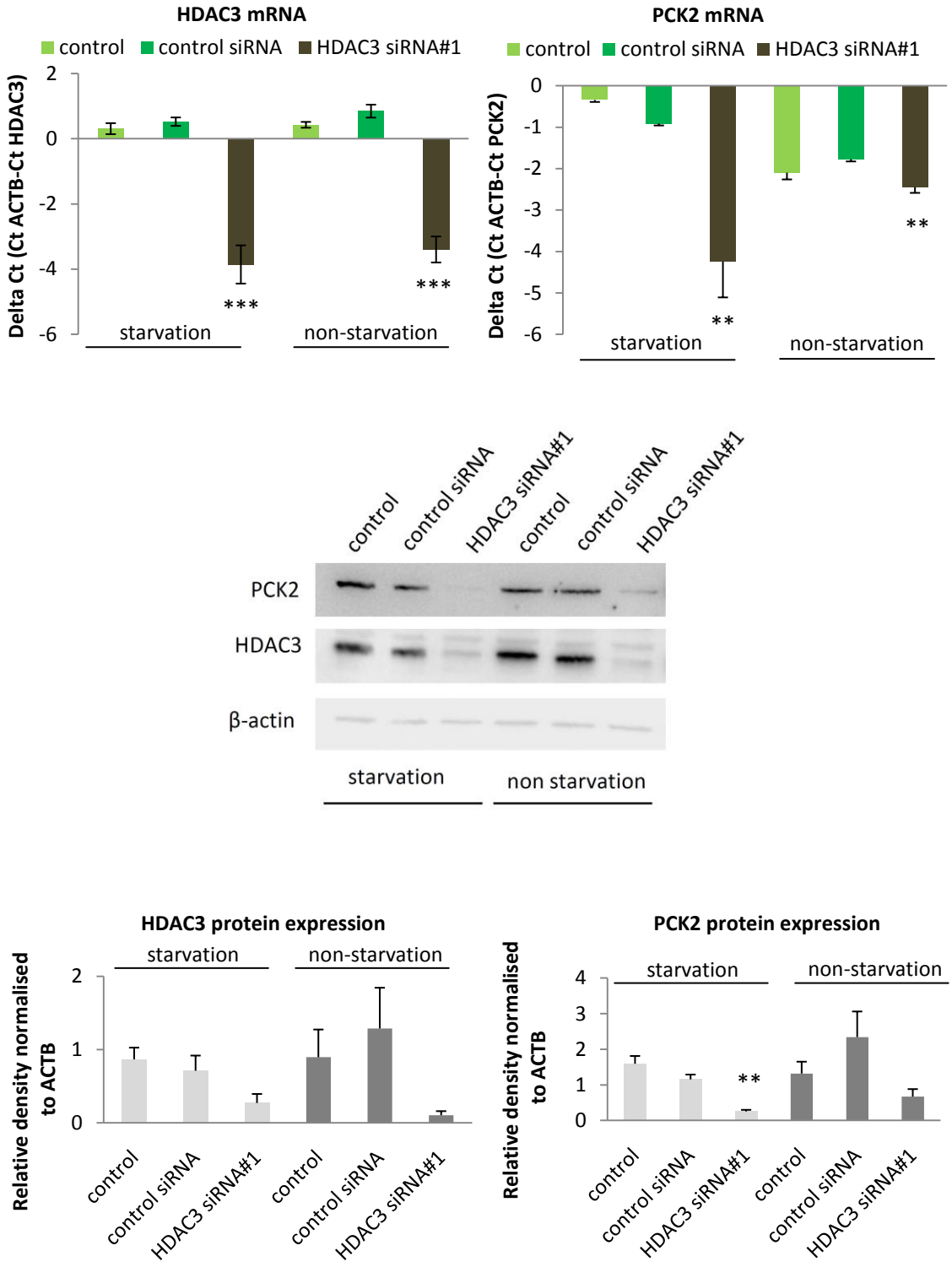

Figure 19: HDAC3 silencing in starvation and non-starvation medium. A549 cells were plated in DMEM/F12 complete. After 24 hours cells were transfected with 40 nM HDAC3 siRNA#1 or control siRNA. The controls were not transfected cells. Another 24 hours later medium was changed. Twenty-four hours later cells were washed with PBS to remove the glucose and FCS. Cells were cultured for two days in starvation or non-starvation medium. Medium was changed every 24 hours. Cells were collected for Western blot or qPCR. Representative immunoblots are shown. The statistics were made with a t-test.* $p < 0.05$; ** $p < 0.01$; *** $p < 0.001$. All samples were compared to DMSO control. Results are shown as mean +/- SEM from three independent experiments. control, untransfected cells.

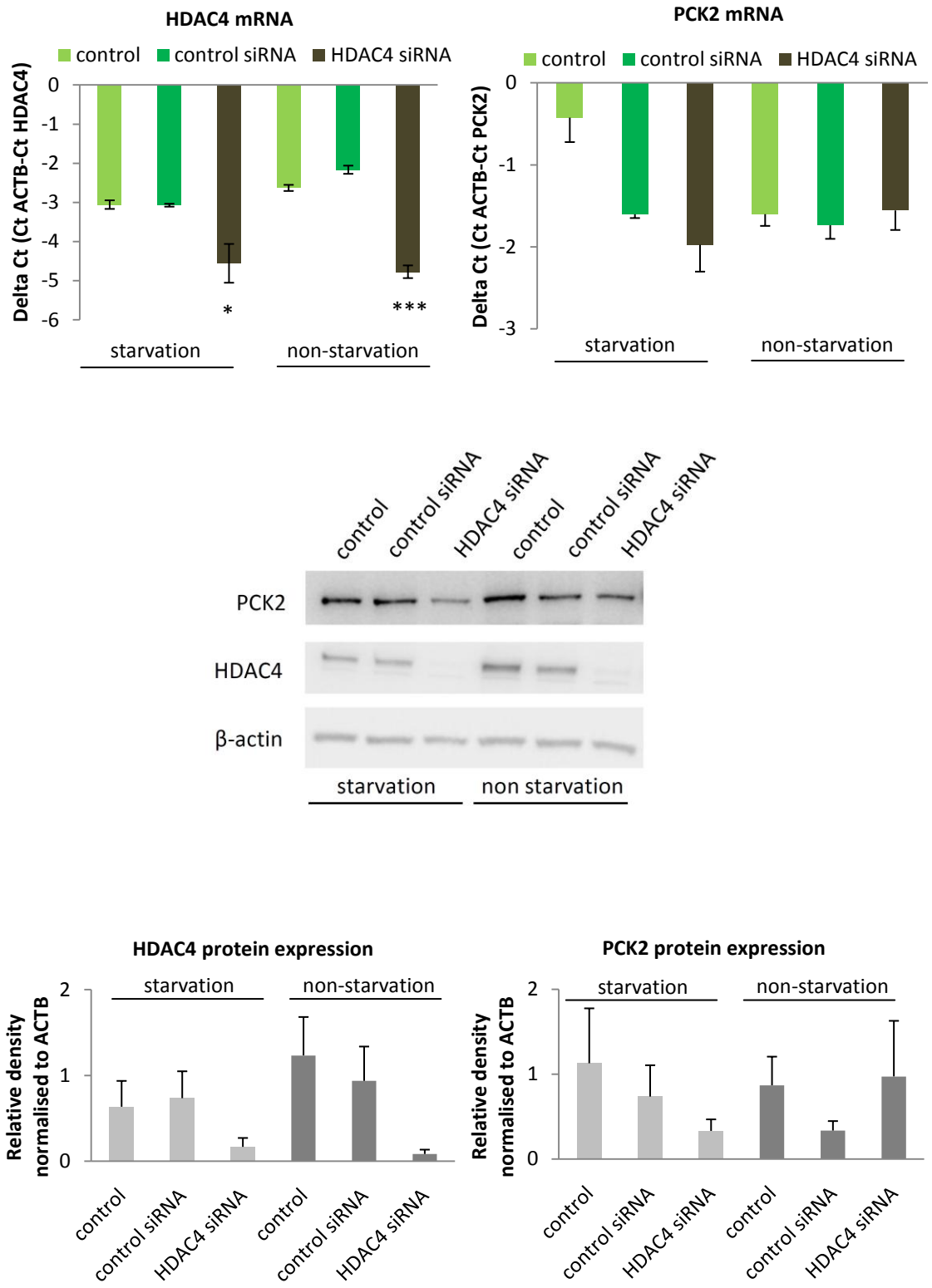

Figure 20: PCK2 mRNA and protein amount after HDAC4 silencing. Cells were transfected and cultured in starvation and non-starvation medium as described before. The statistics were made with a t-test.* $p < 0.05$; ** $p < 0.01$; *** $p < 0.001$. All samples were compared to DMSO control. Results are shown as mean +/- SEM from three independent experiments. Representative immunoblots are shown. n = 3; control, untransfected cells.

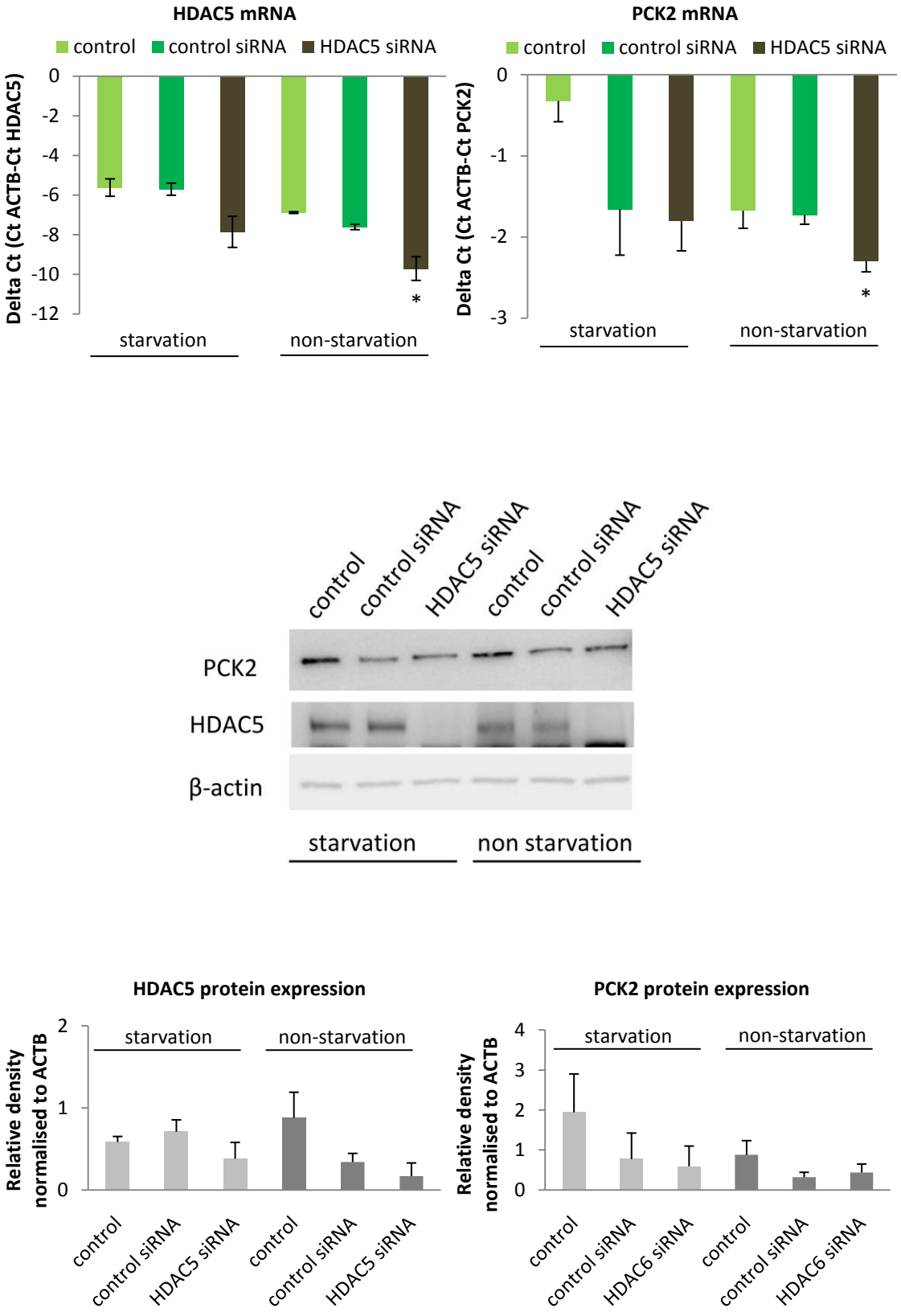

Figure 21: HDAC5 silencing under starvation and non-starvation condition. A549 cells were transfected and cultured in starvation and non-starvation medium as described before. The statistics were made with a t-test.* $p < 0.05$; ** $p < 0.01$; *** $p < 0.001$. All samples were compared to DMSO control. Results are shown as mean +/- SEM from three independent experiments. n = 3; control, untransfected cells.

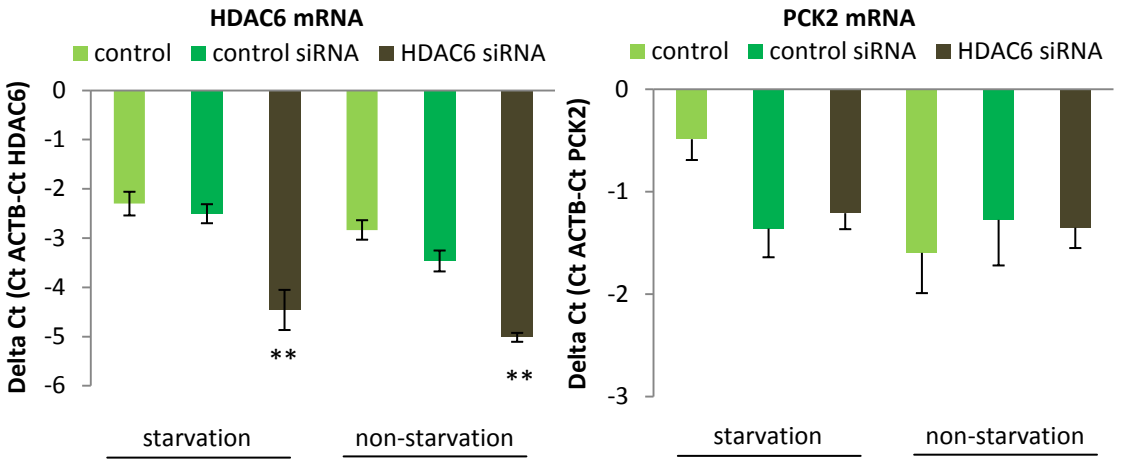

Figure 22: PCK2 mRNA was analyzed after HDAC6 silencing. The cultivation and transfection was done as described before. The statistics were made with a t-test.* $p < 0.05$; ** $p < 0.01$; *** $p < 0.001$. All samples were compared to DMSO control. Results are shown as mean +/- SEM from three independent experiments. n = 3; control, untransfected cells.

Table 11: Summary of HDAC silencing effects on PCK2 under starvation and non-starvation conditions. Red arrows show significant effects.

HDAC	starvation		non-starvation	
	mRNA	protein	mRNA	protein
HDAC3	↓	↓	↓	↔
HDAC4	↔	↔	↔	↔
HDAC5	↔	↔	↓	↔
HDAC6	↔	↔	↔	↔

4.7.3. Combination of HDAC3 and HDAC4 silencing showed no additive or synergistic effects

HDAC3 and HDAC4 can build a complex by interacting via NCoR/SMRT (Fischle et al., 2002). We saw significant effects on the PCK2 expression after HDAC3 silencing and a tentative lowering of the PCK2 amount after HDAC4 silencing. In order to investigate potential additive or synergistic effects of these two HDACs we decided to silence both of them at the same time. The combination of HDAC3 and 4 silencing influenced the PCK2 expression under starvation conditions (Figure 23). However, we did not observe any additive or synergistic effects when we compared the effect of the combined silencing of

HDAC3 and HDAC4 to the silencing of the individual HADCs (Figure 19, 20).

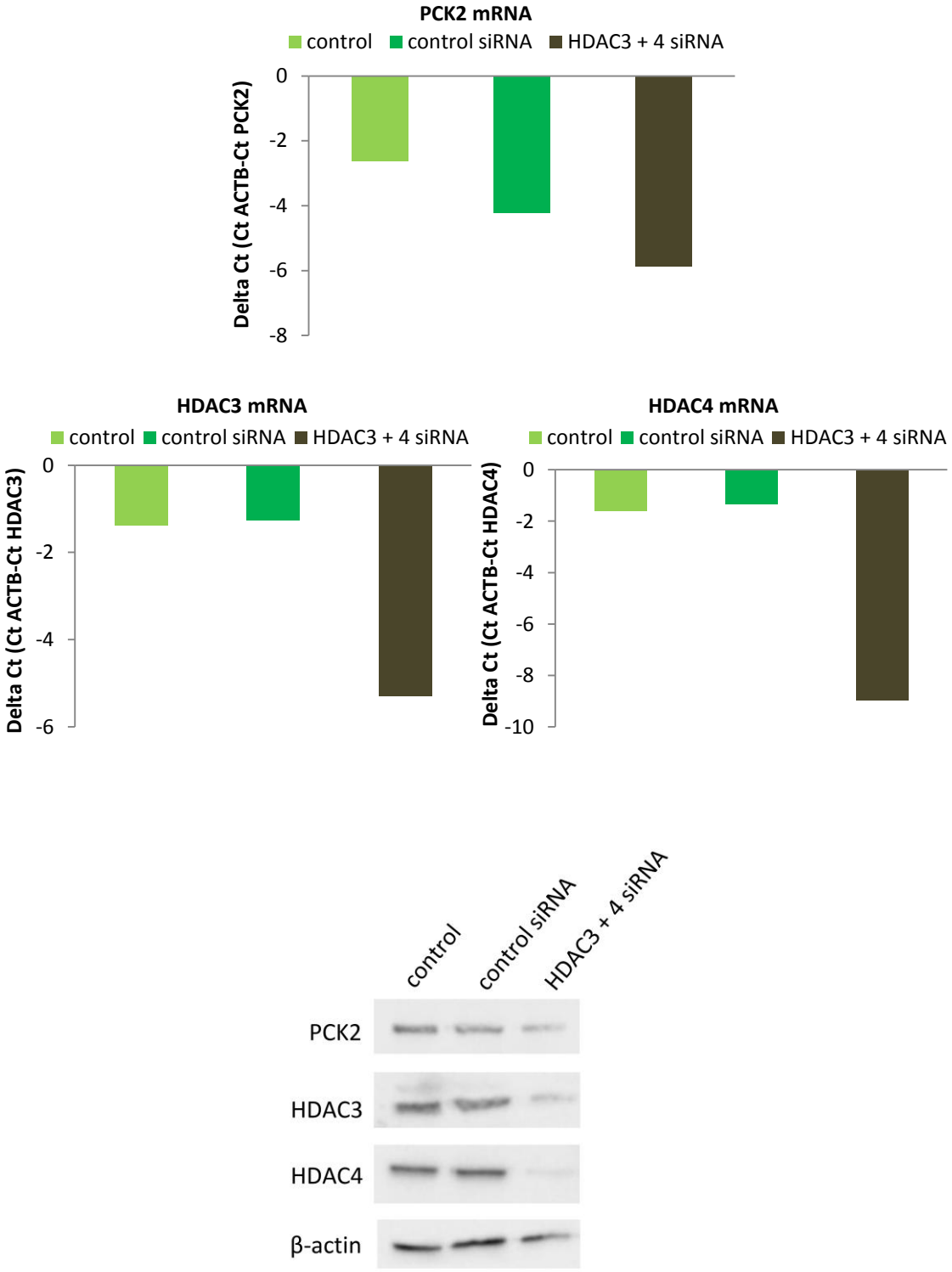

Figure 23: Combined silencing of HDAC3 and HDAC4 under starvation conditions. A549 cells were cultured in DMEM/F12 complete medium for 24 hours before transfection with HDAC3 and HDAC4 siRNAs (40 nm from each siRNA, 80 nm of control siRNA). After 24 hours medium was changed. Another 24 hours later the cells were cultured in starvation medium. After another 24 hours the medium was changed. Cells were collected for Western blot and qPCR. HDAC3 siRNA#1 was used for these experiments. n = 2, control, untransfected cells.

4.7.4. HDAC3 silencing with siRNA#2 showed no changes of the mRNA or protein amount of PCK2

To verify the results from the HDAC3 silencing, an additional HDAC3 siRNA from a different company was used (further referred as HDAC3 siRNA#2). As for the other HDACs we performed a pilot experiment to check the silencing effects after 48 hours. The HDAC3 knockdown after 48 hours was about 80% (Figure 24 A) compared to control cells.

To analyze the effect of HDAC3 siRNA#2 silencing on PCK2 cells were cultured under starvation conditions after the transfection. SiRNA#2 was used at a concentration of 40 nM. The effects of HDAC3 silencing with siRNA#2 on PCK2 mRNA were highly variable. There were no effects on the protein level. Representative Western blots are shown in Figure 24 B. Control siRNA from the same company led to unexpected inhibition of PCK2 protein (data not shown) and, thus, was replaced by control siRNA used in the previous experiments. SiRNA used in all previous experiments is chemically modified to reduce off-target effects, while siRNA#2 (both, control and HDAC3 siRNA) is not chemically modified. This raises the question, whether cells are stressed by off-target effects of the unmodified siRNA#2.

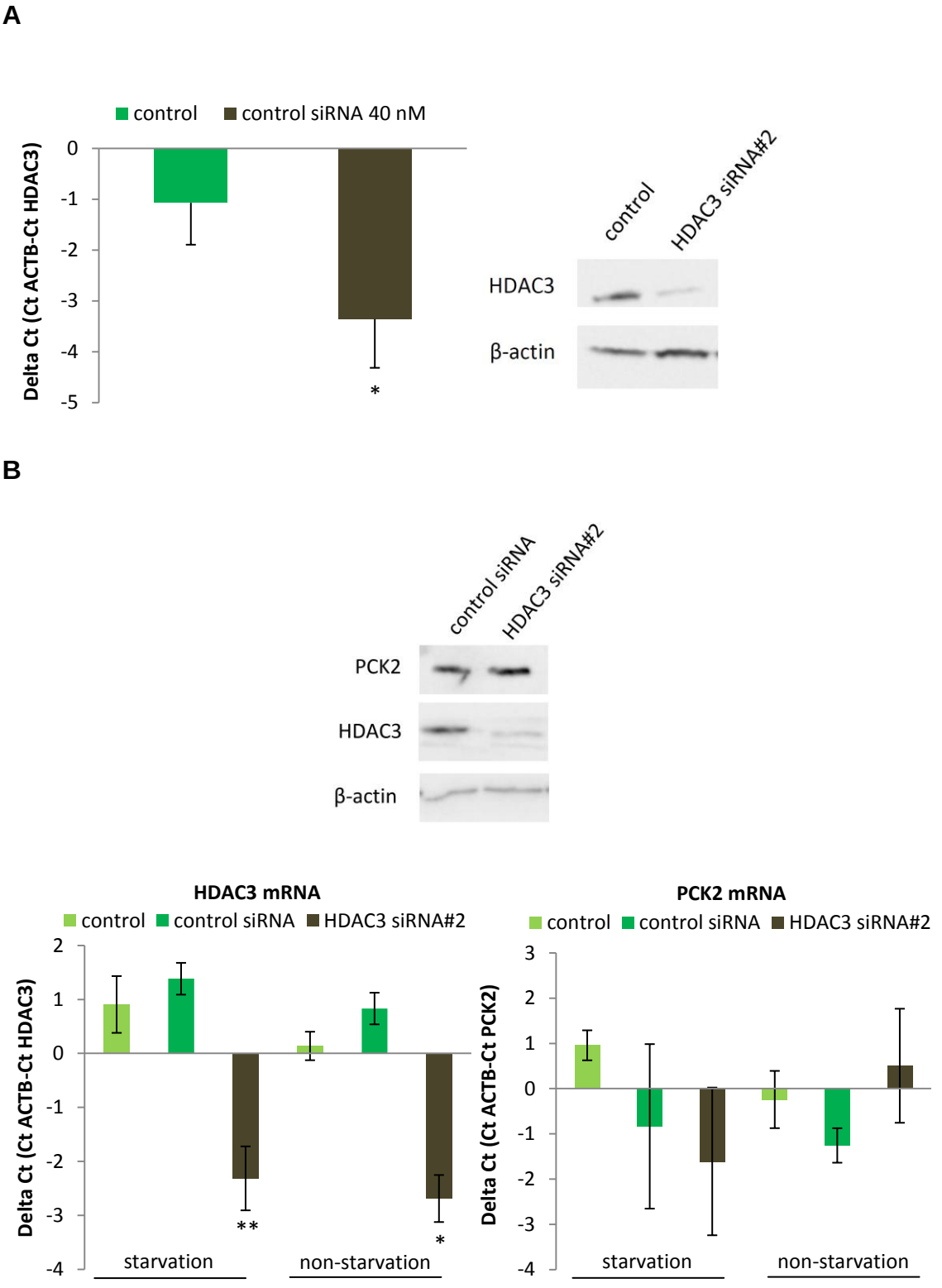

Figure 24: Effects of HDAC3 siRNA#2 silencing on PCK2 expression. (A) After 24 hours in DMEM/F12 complete medium cells were transfected with control siRNAs or HDAC3 siRNA#2. The final siRNA concentration was 40 nM. Cells were collected 48 hours after transfection and Western blot or qPCR was performed. (B) Cells were transfected and cultured under starvation conditions as described before. The statistics were made with a t-test.* $p < 0.05$; ** $p < 0.01$; *** $p < 0.001$. All samples were compared to DMSO control. Representative immunoblots are shown. Results are shown as mean +/- SEM from three independent experiments. control, untransfected cells.

4.8. Cell treatments with specific HDAC inhibitors

4.8.1. LMK235 did not influence PCK2 protein expression under starvation conditions

The pan-HDAC inhibitor panobinostat reduced PCK2 expression. As a second approach to analyze in more detail which HDAC (or which class of HDACs) regulates PCK2, we used the LMK235, a specific HDAC4 and HDAC5 inhibitor. After treatment of A549 cells with LMK235 (concentration range from 50 to 400 nM) no significant reduction of PCK2 expression was observed (Figure 25).

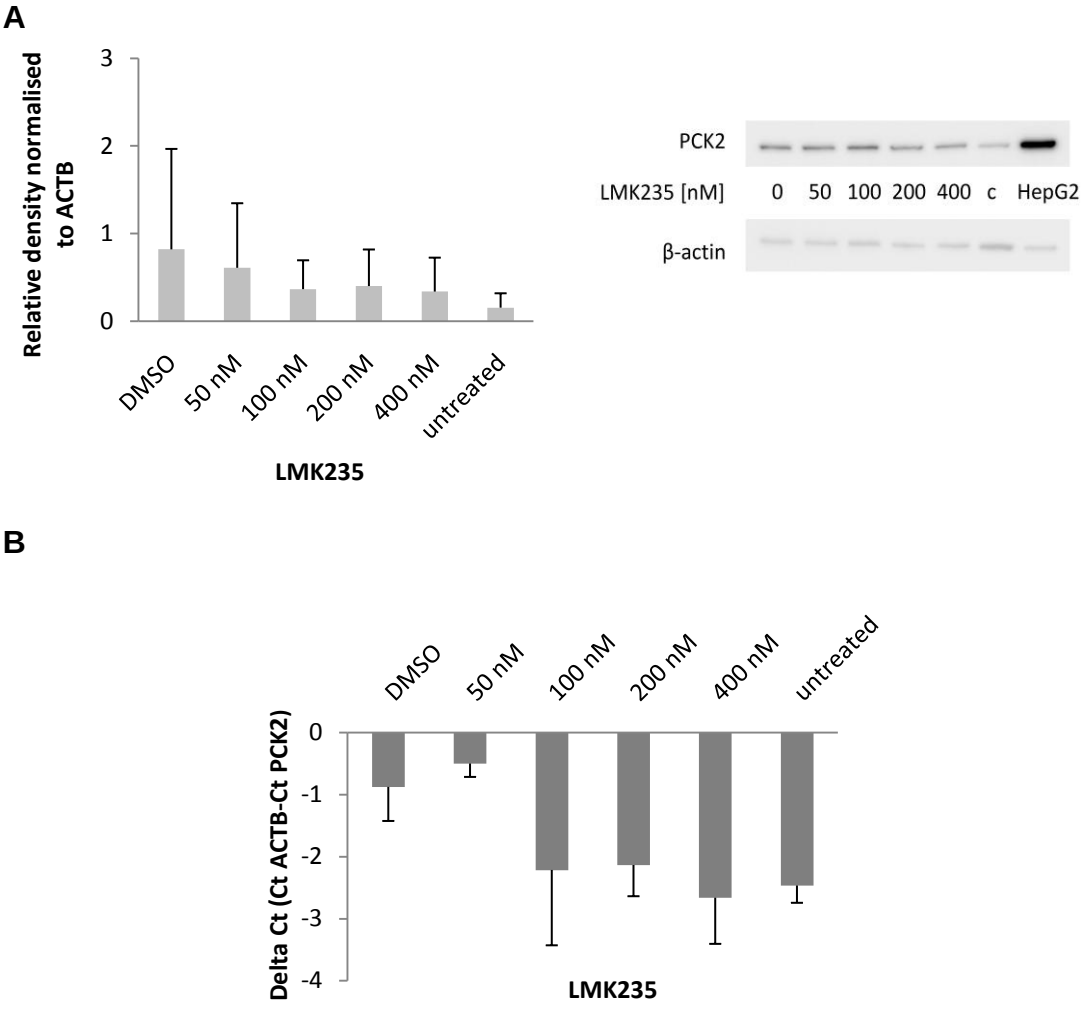

Figure 25: PCK2 expression in A549 cell treated with LMK235 under starvation conditions. Cells were plated in medium with 10 mM glucose and 10% FCS. After 24 hours cells were treated with different LMK235 concentrations or with vehicle control DMSO in starvation medium for another 48 hours. (A). QPCR results and representative immunoblots are shown. Beta-actin was used as a loading control. (B) Relative density of PCK2 signals normalized to beta-actin (ACTB). Results are shown as mean +/- SEM from three independent experiments. FCS, fetal calf serum.

4.8.2. RGFP966 treatment did not influence the PCK2 amount in A549 cells

HDAC3 silencing showed a significant reduction of PCK2 mRNA and protein amount. To verify these results RGFP966, a specific HDAC3 inhibitor was used. A549 cells were treated for 24 hours with this inhibitor. We used concentrations and incubation times as previously described by others (Wells et al., 2013). However, there were no visible effects of RGFP966 on the PCK2 protein amount (Figure 26).

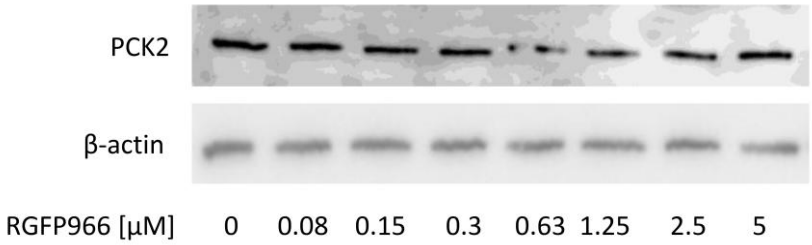

Figure 26: RGFP966 had no effects on PCK2 amount in A549 cells. Cells were plated in DMEM/F12 complete for 24 hours. Then cells were incubated for 24 hours in starvation or non-starvation media with different RGFP966 concentrations. Western blot shows PCK2 protein amount in A549 cells treated for 24 hours with RGFP966 in starvation medium.

5. Discussion

For proliferating cells, like tumors cells, glucose is an important nutrient to generate ATP and macromolecules (Vander Heiden et al., 2009). A lack of glucose leads to metabolic stress in cancer cells (Vincent et al., 2015). Under low glucose conditions the gluconeogenesis enzyme PCK2 has recently been shown to play an important role in the metabolic adaptation of lung cancer cells. In two lung adenocarcinoma cell lines, A549 and NCI-H23, PCK2 expression is upregulated under low glucose conditions (Leithner et al., 2015). Furthermore, PCK2 expression is crucial for tumor growth *in vivo* (Vincent et al., 2015) and an increased PCK2 expression was found in human NSCLC tumor tissues (Vincent et al., 2015; Leithner et al., 2015). Because of that, the gluconeogenesis enzyme PCK2 might be a potential target for cancer therapy (Leithner, 2015).

PCK2 is expressed in most tissues but the highest expression was shown in the liver and kidney (Stark et al., 2014). The PCK2 gene is highly conserved in all eukaryotes, indicating that PCK2 has an important biological role. There is not much known about the regulation of PCK2, in contrast to the cytoplasmic isoform of PEPCK, PCK1. However, present data suggest that PCK2 might have an important role in gluconeogenesis in humans (Stark et al., 2014). In the liver gluconeogenesis genes can be activated by HDAC3 and by class IIa HDACs (Mihaylova et al., 2011).

To investigate the regulatory mechanism of PCK2 in lung cancer cells, we treated A549 cells with panobinostat, a pan-HDAC inhibitor for class I and II HDACs. The acetylation status of histones 3 and 4 was increased in a concentration-dependent manner and these effects were more prominent under starvation conditions. A previous study from our group also showed similar effect in H23 lung cancer cells under standard growth conditions (Fischer et al., 2015). After treatment with panobinostat at nanomolar concentrations histones are hyper-acetylated, which leads to apoptosis in malignant cells (Anne et al., 2013). Our results based on the assay for active caspase 3 and 7 also showed increased apoptosis in A549 cells after panobinostat treatment in DMEM/F12 complete medium. At panobinostat concentrations above 64 nM the percentage of apoptotic cells rose considerably (45% and 53% apoptosis with 128 nM and with 256 nM panobinostat, respectively). Therefore we decided to use

concentrations up to 64 nM for our experiments. Furthermore, the cells are more sensitive to panobinostat under starvation conditions then under non-starvation conditions (Figure 12). Our experiments showed that panobinostat inhibited PCK2 protein and mRNA levels in a concentration-dependent manner, especially under low glucose and FCS starvation conditions. In the absence of FCS the effects of glucose and panobinostat on PCK2 expression were more prominent. The reason for this is unclear and the explanation has a speculative character. In FCS there might be some compounds which influence gluconeogenesis, like e.g. some lipids which can regulate PCK2. For example, one of these regulatory lipids is all-trans retinoic acids that can regulate PCK1 (Cadoudal et al., 2008). Taken together, our experiments showed that panobinostat inhibits PCK2 expression under starvation conditions, likely by inhibiting gene transcription. These results indicate that HDACs play a role in the regulation of PCK2.

To investigate the role of individual HDACs in the regulation of PCK2 we silenced HDACs under different media conditions. Our pilot experiments showed that 48 hours after the transfection knockdown effects reached more than 70%. In order to exclude off-target effects we checked the siRNA sequences for their homology with the target mRNA and with all known gene sequences by using the blast function from NCBI. The e-values for specific sequence-blast were always below 0.05, thus indicating high sequence specificity of siRNA molecules.

Mihaylova et al. described the role of HDACs in the regulation of gluconeogenesis in the liver. Under fasting conditions class IIa HDACs (which includes HDAC4 and 5) have been shown to get activated and to recruit HDAC3 complexed with nuclear receptor corepressor (NCoR). Consequently, HDAC3 deacetylated the transcription factor FOXO, which led to transcription of the gluconeogenesis genes PEPCK and glucose-6-phospahtase (Mihaylova et al., 2011). In other studies it has also been shown that HDAC3 can activate transcription and interact with non-histone target proteins (Fischle et al., 2002). HDAC1, 2 and 3 have similar functions. For example HDAC1, 2 and 3 containing complexes can act as corepressors for transcriptional repressors (Yang et al., 2003). In our study silencing of HDAC1 and 2 had no influence on

PCK2 protein and mRNA levels. In contrast, HDAC3 silencing showed a significant reduction of the PCK2 expression both on mRNA and on protein level under starvation conditions. To verify this results obtained with the HDAC3 siRNA#1 set, a second siRNA set from another company was used (HDAC3 siRNA#2). Silencing of HDAC3 with HDAC3 siRNA#2 showed a tentative but not significant lowering of the PCK2 mRNA level, however the variability between experiments was high. No effects of HDAC3 siRNA#2 on PCK2 protein levels were found. The knockdown effects of HDAC3 siRNA#2 were about 15% lower than of HDAC3 siRNA#1. This might explain the missing effects on PCK2 protein level. Control siRNA#2 from the same company as HDAC3 siRNA#2 led to unexpected inhibition of PCK2 protein (data not shown), which might indicate some off-target effects. Thus, it was replaced by control siRNA used in all other experiments, which is chemically modified to reduce off-target effects. In contrast, siRNA#2 (both, control and HDAC3 siRNA) is not chemically modified. This raises the question, whether cells are stressed by off-target effects, e.g. the innate immune response, of the unmodified siRNA#2. Additional experiments with an independent set of HDAC3 siRNA which is modified to minimize off-target effects or with HDAC3 shRNA are planned.

The specificity of the effects of HDAC3 silencing on PCK2 expression is further questioned by the lack of an effect of RGFP966, a specific HDAC3 inhibitor. However, we do not know if HDAC3 activity in A549 lung cancer cells was influenced by RGFP966 at the applied concentrations. To answer this question, an activity assay for HDAC3 should be performed. In many silencing experiments an effect of transfection with control (non-silencing) siRNA on PCK2 protein, compared to untreated control cells, was observed. These results suggest that the transfection itself may influence cellular metabolism. That may also explain different results observed after transfections with two different HDAC3 siRNAs and by an HDAC3 inhibitor alone. However, present literature data indicate that HDAC3 might be an important protein in cancer cells. In squamous cell lung carcinomas the HDAC3 mRNA and protein amount was increased (Karagianni et al., 2007). HDAC3 silencing in colon cancer cells induced apoptosis and stopped the proliferation (Karagianni et al., 2007). Therefore, it is definitely worthwhile to further investigate and clarify the role of HDAC3 in the metabolism of lung cancer cells.

HDAC4 silencing showed a tentative lowering of the PCK2 protein amount under starvation conditions, although these effects were not significant. HDAC3 and HDAC4 predominantly reduced PCK2 expression under starvation conditions. The reason might be the higher PCK2 expression under starvation conditions; since PCK2 may provide intermediates for tumor cell proliferation and survival in low glucose environment (Balsa-Martinez et al., 2015; Leithner et al., 2015; Vincent et al., 2015). It was shown that HDAC3 and HDAC4 can interact with each other via NCoR/SMRT (Fischle et al., 2002). In our study the double-silencing of HDAC3 and 4 did not show a stronger effect then the HDAC3 or HDAC4 silencing separately. Although it has been described that HDAC5 is also able to interact with the NCoR complex (Guenther et al., 2001), in our experiment there were no visible effects of HDAC5 silencing on PCK2 mRNA or protein amount. We also performed experiments with LMK235, a specific HDAC4 and HDAC5 inhibitor. LMK235 was applied in a range of concentrations used in other studies (Li et al., 2016). However, this inhibitor showed no reduction of PCK2 mRNA or protein amount under starvation conditions. It was shown that HDAC6 is important for the gluconeogenesis in liver. The inhibition of HDAC6 with pharmacological substances lowers the glucocorticoid induced PEPCK expression (Winkler et al., 2012). Interestingly, in our experiment HDAC6 silencing did not influence the expression of PCK2.

The activity of HDACs correlates with the amount of acetyl-CoA. It would be important to know more about the changes of the acetylation status in the cell under starvation conditions. Chromatin modifications in the organism are dependent on the environment of the cells (Etchegaray et al., 2016). Cells have to adapt their metabolism to survive under different growth conditions. The enzymes responsible for these chromatin modifications are dependent on cofactors like acetyl-CoA, ATP and NAD^+. Acetyl-CoA is used by HATs to acetylate histones. The availability of acetyl-CoA and the activity of HATs are correlated in mammalian cells. Acetyl-CoA is an important regulator of the metabolic status in the cell (Jiang et al., 2011). Under starvation conditions β-oxidation produces acetyl-CoA to fuel the TCA cycle. High acetyl-CoA levels promote the acetylation of histones, so the gene expression is increased under

high nutrient amount conditions. Since the action of HATs and HDACs is dependent on acetyl-CoA levels they can be regarded as sensors for the availability of nutrients (Etchegaray et al., 2016). It was shown that under high glucose conditions PCK1 is destabilized by acetylation by the P300 acetyltransferase (Xiong et al., 2011; Jiang et al., 2011). That further supports our theory that PCK2 is regulated by HDACs and HATs.

In summary we found that a pan-HDAC inhibitor, panobinostat, significantly reduced PCK2 expression in A549 lung cancer cells. Systematic silencing experiments of 6 different HDACs suggested that HDAC3 (and probably HDAC4) are the responsible HDACs for regulation of PCK2, however these results have to be verified with other methods. Further studies will be necessary to learn more about PCK2 and its regulation.

6. References

Alberg, A. J., Brock, M. V., Ford, J. G., Samet, J. M., & Spivack, S. D. (2013). Epidemiology of lung cancer: Diagnosis and management of lung cancer, 3rd ed: American College of chest physicians evidence-based clinical practice guidelines. *Chest*, *143*(5), 1–29. http://doi.org/10.1378/chest.12-2345

Alberg, A. J., & Samet, J. (2003). Epidemiology of lung cancer. *Chest*, *123*(1), 21–49. http://doi.org/10.1378/chest.123.1

Anne, M., Sammartino, D., Barginear, M. F., & Budman, D. (2013). Profile of panobinostat and its potential for treatment in solid tumors: An update. *OncoTargets and Therapy*, *6*, 1613–1624. http://doi.org/10.2147/OTT.S30773

Bailey, H., Stenehjem, D. D., & Sharma, S. (2015). Panobinostat for the treatment of multiple myeloma: The evidence to date. *Journal of Blood Medicine*, *6*, 269–276. http://doi.org/10.2147/JBM.S69140

Balsa-Martinez, E., & Puigserver, P. (2015). Cancer cells hijack gluconeogenic enzymes to fuel cell growth. *Molecular Cell*, *60*(4), 509–511. http://doi.org/10.1016/j.molcel.2015.11.005

Bender, T., & Martinou, J. (2016). The mitochondrial pyruvate carrier in health and disease: To carry or not to carry? *Biochimica et Biophysica Acta (BBA) - Molecular Cell Research*, *2*(10), 881–898. http://doi.org/10.1016/j.bbamcr.2016.01.017

Cadoudal, T., Glorian, M., Massias, A., Fouque, F., Forest, C., & Benelli, C. (2008). Retinoids upregulate phosphoenolpyruvate carboxykinase and glyceroneogenesis in human and rodent adipocytes. *The Journal of Nutrition*, *138*(6), 1004–1009.

Cairns, R. A., Harris, I. S., & Mak, T. W. (2011). Regulation of cancer cell metabolism. *Nature Reviews. Cancer*, *11*(2), 85–95. http://doi.org/10.1038/nrc2981

Cantor, J. R., & Sabatini, D. M. (2012). Cancer cell metabolism: One hallmark, many faces. *Cancer Discovery*. http://doi.org/10.1158/2159-8290.CD-12-0345

Cheng, Z., & White, M. F. (2012). The Aktion in non-canonical insulin signaling. *Nat Med*, *18*(3), 351–353. http://doi.org/nm.2694 [pii]\r10.1038/nm.2694

Cheung, P., & Lau, P. (2005). Epigenetic Regulation by Histone Methylation and Histone Variants. *Molecular Endocrinology*, *19*(3), 563–573. http://doi.org/10.1210/me.2004-0496

Crisanti, M. C., Wallace, A. F., Kapoor, V., Vandermeers, F., Dowling, M. L., Pereira, L. P., … Albelda, S. M. (2013). The HDAC inhibitor panobinostat (LBH589) inhibits mesothelioma and lung cancer cells in vitro and in vivo with particular efficacy for small cell lung cancer. *American Association for Cancer Research*, *8*(8), 2221–2231.

http://doi.org/10.1016/j.cmet.2012.08.002.

Du, X., Crawford, D. L., Nacci, D. E., & Oleksiak, M. F. (2016). Heritable oxidative phosphorylation differences in a pollutant resistant fundulus heteroclitus population. *Aquatic Toxicology*, *177*, 44–50. http://doi.org/10.1016/j.aquatox.2016.05.007

Etchegaray, J. P., & Mostoslavsky, R. (2016). Interplay between metabolism and epigenetics: A nuclear adaptation to environmental changes. *Molecular Cell*, *62*(5), 695–711. http://doi.org/10.1016/j.molcel.2016.05.029

Fischer, C., Leithner, K., Wohlkoenig, C., Quehenberger, F., Bertsch, A., Olschewski, A., … Hrzenjak, A. (2015). Panobinostat reduces hypoxia-induced cisplatin resistance of non-small cell lung carcinoma cells via HIF-1α destabilization. *Molecular Cancer*, *14*(4). http://doi.org/10.1186/1476-4598-14-4

Fischle, W., Dequiedt, F., Hendzel, M. J., Guenther, M. G., Lazar, M. A., Voelter, W., & Verdin, E. (2002). Enzymatic activity associated with class II HDACs is dependent on a multiprotein complex containing HDAC3 and SMRT/N-CoR. *Molecular Cell*, *9*(1), 45–57. http://doi.org/10.1016/S1097-2765(01)00429-4

Garcia-Calvo, M., Peterson, E. P., Rasper, D. M., Vaillancourt, J. P., Zamboni, R., Nicholson, D. W., & Thornberry, N. A. (1999). Purification and catalytic properties of human caspase family members. *Cell Death and Differentiation*, *6*(4), 362–369. http://doi.org/10.1038/sj.cdd.4400497

Greve, G., Schiffmann, I., Pfeifer, D., Pantic, M., Schüler, J., & Lübbert, M. (2015). The pan-HDAC inhibitor panobinostat acts as a sensitizer for erlotinib activity in EGFR-mutated and -wildtype non-small cell lung cancer cells. *BMC Cancer*, *15*, 947–957. http://doi.org/10.1186/s12885-015-1967-5

Guenther, M. G., Barak, O., & Lazar, M. A. (2001). The SMRT and N-CoR Corepressors Are Activating Cofactors for Histone Deacetylase 3. *Molecular and Cellular Biology*, *21*(18), 6091–6101. http://doi.org/10.1128/MCB.21.18.6091-6101.2001

Haberland, M., Montgomery, R. L., & Olson, E. N. (2009). The many roles of histone deacetylases in development and physiology: Implications for disease and therapy. *Nature Reviews. Genetics*, *10*(1), 32–42. http://doi.org/10.1038/nrg2485

Han, H., Kang, G., Kim, J. S., Choi, B. H., & Koo, S. (2016). Regulation of glucose metabolism from a liver-centric perspective. *Experimental & Molecular Medicine*, *48*, 218–228. http://doi.org/10.1038/emm.2015.122

Hanahan, D., & Weinberg, R. A. (2011). Hallmarks of cancer: The next generation. *Cell*, *144*(5), 646–674. http://doi.org/10.1016/j.cell.2011.02.013

Hanna, J. M., & Onaitis, M. W. (2013). Cell of origin of lung cancer. *Journal of Carcinogenesis*, *12*, 6. http://doi.org/10.4103/1477-3163.109033

Hansen, F. K., Sumanadasa, S. D. M., Stenzel, K., Duffy, S., Meister, S.,

Marek, L., … Kurz, T. (2014). Discovery of HDAC inhibitors with potent activity against multiple malaria parasite life cycle stages. *European Journal of Medicinal Chemistry*, *82*, 204–213. http://doi.org/10.1016/j.ejmech.2014.05.050

Herbst, R. S., Heymach, J. V, & Lippman, S. M. (2008). Lung cancer. *The New England Journal of Medicine*, *359*(13), 1367–1380. http://doi.org/10.1056/NEJMra0802714

Holbert, M. A., & Marmorstein, R. (2005). Structure and activity of enzymes that remove histone modifications. *Current Opinion in Structural Biology*, *15*(6), 673–680. http://doi.org/10.1016/j.sbi.2005.10.006

Jiang, W., Wang, S., Xiao, M., Lin, Y., Zhou, L., Lei, Q., … Zhao, S. (2011). Acetylation regulates gluconeogenesis by promoting PEPCK1 degradation via recruiting the UBR5 ubiquitin ligase. *Molecular Cell*, *43*(1), 33–44. http://doi.org/10.1016/j.molcel.2011.04.028

Karagianni, P., & Wong, J. (2007). HDAC3: Taking the SMRT-N-CoRrect road to repression. *Oncogene*, *26*(37), 5439–5449. http://doi.org/10.1038/sj.onc.1210612

Koinis, F., Kotsakis, A., & Georgoulias, V. (2016). Small cell lung cancer (SCLC): No treatment advances in recent years. *Translational Lung Cancer Research*, *5*(1), 39–50. http://doi.org/10.3978/j.issn.2218-6751.2016.01.03

Kozera, B., & Rapacz, M. (2013). Reference genes in real-time PCR. *Journal of Applied Genetics*, *54*(4), 391–406. http://doi.org/10.1007/s13353-013-0173-x

Kuida, K., Zheng, T. S., Na, S., Kuan, C.-Y., Yang, D., Karasuyama, H., … Flavell, R. A. (1996). Decreased apoptosis in the brain and premature lethality in CPP32-deficient mice. *Nature*, *384*, 368–372. http://doi.org/10.1038/384368a0

Laubach, J. P., Moreau, P., San-Miguel, J. F., & Richardson, P. G. (2015). Panobinostat for the treatment of multiple myeloma. *Clinical Cancer Research*, *21*(21), 4767–73. http://doi.org/10.1158/1078-0432.CCR-15-0530

Leithner, K. (2015). PEPCK in cancer cell starvation. *Oncoscience*, *2*(10), 805–806.

Leithner, K., Hrzenjak, A., Trötzmüller, M., Moustafa, T., Köfeler, H. C., Wohlkoenig, C., … Olschewski, H. (2015). PCK2 activation mediates an adaptive response to glucose depletion in lung cancer. *Oncogene*, *34*(8), 1044–1050. http://doi.org/10.1038/onc.2014.47

Lemoine, M., Derenzini, E., Buglio, D., Medeiros, L. J., Davis, R. E., Zhang, J., … Younes, A. (2012). The pan-deacetylase inhibitor panobinostat induces cell death and synergizes with everolimus in Hodgkin lymphoma cell lines. *Blood Journal*, *119*(17), 4017–4025. http://doi.org/10.1182/blood-2011-01-331421

Li, A., Liu, Z., Li, M., Zhou, S., Xu, Y., & Xiao, Y. (2016). HDAC5, a potential therapeutic target and prognostic biomarker, promotes proliferation , invasion and migration in human breast cancer. *Oncotarget*, *10*. http://doi.org/10.18632/oncotarget.9274

Li, X.-B., Gu, J.-D., & Zhou, Q.-H. (2015). Review of aerobic glycolysis and its key enzymes - new targets for lung cancer therapy. *Thoracic Cancer*, *6*(1), 17–24. http://doi.org/10.1111/1759-7714.12148

Liberti, M. V., & Locasale, J. W. (2016). The Warburg effect: How does it benefit cancer cells? *Trends in Biochemical Sciences*, *41*(3), 211–218. http://doi.org/10.1016/j.tibs.2015.12.001

Lu, X., Wang, L., Yu, C., Yu, D., & Yu, G. (2015). Histone acetylation modifiers in the pathogenesis of Alzheimer's disease. *Frontiers in Cellular Neuroscience*, *9*(226). http://doi.org/10.3389/fncel.2015.00226

Malvaez, M., McQuown, S. C., Rogge, G. a, Astarabadi, M., Jacques, V., Carreiro, S., … Wood, M. a. (2013). HDAC3-selective inhibitor enhances extinction of cocaine-seeking behavior in a persistent manner. *Proceedings of the National Academy of Sciences of the United States of America*, *110*(7), 2647–2652. http://doi.org/10.1073/pnas.1213364110

Méndez-Lucas, A., Hyroššová, P., Novellasdemunt, L., Viñals, F., & Perales, J. C. (2014). Mitochondrial PEPCK is a Pro-Survival, ER-Stress Response Gene Involved in Tumor Cell Adaptation to Nutrient Availability. *The Journal of Biological Chemistry*, *289*(32), 22090–22102. http://doi.org/10.1074/jbc.M114.566927

Mihaylova, M. M., & Shaw, R. J. (2013). Metabolic reprogramming by class I and II histone deacetylases. *Trends in Endocrinology and Metabolism*, *24*(1), 48–57. http://doi.org/10.1016/j.tem.2012.09.003

Mihaylova, M. M., Vasquez, D. S., Ravnskjaer, K., Denechaud, P. D., Yu, R. T., Alvarez, J. G., … Shaw, R. J. (2011). Class IIa histone deacetylases are hormone-activated regulators of FOXO and mammalian glucose homeostasis. *Cell*, *145*(4), 607–621. http://doi.org/10.1016/j.cell.2011.03.043

Murakami, Y. (2002). Functional cloning of a tumor suppressor gene, TSLC1, in human non-small cell lung cancer. *Oncogene*, *21*(45), 6936–48. http://doi.org/10.1038/sj.onc.1205825

Polanski, B., J.-P., J., R., & M., C. (2016). Quality of life of patients with lung cancer. *OncoTargets and Therapy*, *9*, 1023–1028. http://doi.org/10.2147/OTT.S100685

Polet, F., & Feron, O. (2013). Endothelial cell metabolism and tumour angiogenesis: Glucose and glutamine as essential fuels and lactate as the driving force. *Journal of Internal Medicine*, *273*(2), 156–165. http://doi.org/10.1111/joim.12016

Ramalingam, S. S., Owonikoko, T. K., & Khuri, F. R. (2011). Lung Cancer: New biological insights and recent therapeutic advances. *Cancer*, *61*(2), 91–

112. http://doi.org/10.3322/caac.20102.Available

Roviello, G. (2015). The distinctive nature of adenocarcinoma of the lung. *OncoTargets and Therapy*, *8*, 2399–2406. http://doi.org/10.2147/OTT.S89225

Schulze, A., & Harris, A. L. (2012). How cancer metabolism is tuned for proliferation and vulnerable to disruption. *Nature*, *491*(7424), 364–73. http://doi.org/10.1038/nature11706

Sekido, Y., Fong, K. M., & Minna, J. D. (2003). Molecular genetics of lung cancer. *Annual Review of Medicine*, *54*, 73–87. http://doi.org/10.1146/annurev.med.54.101601.152202

Stark, R., & Kibbey, R. G. (2014). The mitochondrial isoform of phosphoenolpyruvate carboxykinase (PEPCK-M) and glucose homeostasis: Has it been overlooked? *Biochimica et Biophysica Acta - General Subjects*, *1840*(4), 1313–1330. http://doi.org/10.1016/j.bbagen.2013.10.033

Thermo Fisher. (2016). Retrieved from https://www.thermofisher.com/order/catalog/product/C10423

Urbánek, P., & Klotz, L.-O. (2016). Posttranscriptional regulation of FOXO expression: MicroRNAs and beyond. *British Journal of Pharmacology*, *253*(17). http://doi.org/10.1111/bph.13471

Vander Heiden, M., Cantley, L., & Thompson, C. (2009). Understanding the Warburg effect: The metabolic requiremetns of cell proliferation. *Science*, *324*(5930), 1029–1033. http://doi.org/10.1126/science.1160809.Understanding

Vincent, E. E., Sergushichev, A., Griss, T., Gingras, M. C., Samborska, B., Ntimbane, T., … Jones, R. G. (2015). Mitochondrial phosphoenolpyruvate carboxykinase regulates metabolic adaptation and enables glucose-independent tumor growth. *Molecular Cell*, *60*(2), 195–207. http://doi.org/10.1016/j.molcel.2015.08.013

Waclaw, B., Bozic, I., Pittman, M. E., Hruban, R. H., Vogelstein, B., & Nowak, M. a. (2015). A spatial model predicts dispersal and cell turnover cause reduced intra-tumor heterogeneity. *Nature*, *525*(7568), 261–267. http://doi.org/10.1101/016824

Wallace, J. C., & Barritt, G. J. (2001). Gluconeogenesis. *Encyclopedia of Science*. http://doi.org/10.1038/npg.els.0000627

Wells, C. E., Bhaskara, S., Stengel, K. R., Zhao, Y., Sirbu, B., Chagot, B., … Hiebert, S. W. (2013). Inhibition of histone deacetylase 3 causes replication stress in cutaneous T cell lymphoma. *PLoS ONE*, *8*(7), 1–13. http://doi.org/10.1371/journal.pone.0068915

Whittle, N., & Singewald, N. (2014). HDAC inhibitors as cognitive enhancers in fear, anxiety and trauma therapy: where do we stand? *Biochemical Society Transactions*, *42*(2), 569–581. http://doi.org/10.1042/BST20130233

Winkler, R., Benz, V., Clemenz, M., Bloch, M., Foryst-Ludwig, A., Wardat, S., … Kintscher, U. (2012). Histone deacetylase 6 (HDAC6) is an essential modifier of glucocorticoid-induced hepatic gluconeogenesis. *Diabetes*, *61*(2), 513–523. http://doi.org/10.2337/db11-0313

Xiong, Y., Lei, Q. Y., Zhao, S., & Guan, K. L. (2011). Regulation of glycolysis and gluconeogenesis by acetylation of PKM and PEPCK. *Cold Spring Harbor Symposia on Quantitative Biology*, *76*, 285–289. http://doi.org/10.1101/sqb.2011.76.010942

Yang, J., Kalhan, S. C., & Hanson, R. W. (2009). What is the metabolic role of phosphoenolpyruvate carboxykinase? *Journal of Biological Chemistry*, *284*(40), 27025–27029. http://doi.org/10.1074/jbc.R109.040543

Yang, X. J., & Seto, E. (2003). Collaborative spirit of histone deacetylases in regulating chromatin structure and gene expression. *Current Opinion in Genetics and Development*, *13*(2), 143–153. http://doi.org/10.1016/S0959-437X(03)00015-7

7. List of figures

8. List of tables